

2013

Cardioprotective Effects of Mitochondrial-Targeted Antioxidants in Myocardial Ischemia/Reperfusion (I/R) Injury

Regina Ondrasik

Philadelphia College of Osteopathic Medicine, regina.ondrasik@gmail.com

Follow this and additional works at: <http://digitalcommons.pcom.edu/biomed>

 Part of the [Medicine and Health Sciences Commons](#)

Recommended Citation

Ondrasik, Regina, "Cardioprotective Effects of Mitochondrial-Targeted Antioxidants in Myocardial Ischemia/Reperfusion (I/R) Injury" (2013). *PCOM Biomedical Studies Student Scholarship*. Paper 87.

This Thesis is brought to you for free and open access by the Student Dissertations, Theses and Papers at DigitalCommons@PCOM. It has been accepted for inclusion in PCOM Biomedical Studies Student Scholarship by an authorized administrator of DigitalCommons@PCOM. For more information, please contact library@pcom.edu.

Philadelphia College of Osteopathic Medicine
The Graduate Program in Biomedical Sciences
Department of Biomedical Sciences

**Cardioprotective Effects of Mitochondrial-Targeted Antioxidants
in Myocardial Ischemia/Reperfusion (I/R) Injury**

A Thesis in Myocardial Ischemia/Reperfusion Injury by Regina Ondrasik

Submitted in Partial Fulfillment of the Requirements for the Degree of

Master of Science in Biomedical Sciences

July 2013

We approve the thesis of Regina Ondrasik

Lindon H. Young, Ph.D.
Professor of Biomedical Sciences
Thesis Advisor

Robert Barsotti, Ph.D.
Professor of Biomedical Sciences

Ruth Borghaei, Ph.D.
Professor of of Biomedical Sciences

Marcus Bell, Ph.D.
Program Director, Research, Master of Science in Biomedical Sciences

ABSTRACT

Cardioprotective Effects of Mitochondrial-Targeted Antioxidants in Myocardial Ischemia/Reperfusion (I/R) Injury

Reactive oxygen species (ROS) generated during myocardial I/R contribute to post-reperfused cardiac contractile dysfunction. Damaged cardiomyocyte mitochondria are major sites of excess ROS generation during reperfusion. We hypothesized that reducing mitochondrial ROS formation should attenuate myocardial I/R injury and thereby improve function of isolated perfused rat hearts subjected to I(30min)/R(45min) compared to untreated I/R hearts. Mitoquinone (MitoQ, MW=579g/mol; complexed with cyclodextrin (MW=1135g/mol) to improve water solubility, total MW=1714g/mol), a coenzyme Q derivative, and SS-31 (Szeto-Schiller) peptide ((D-Arg)-Dmt-Lys-Phe-Amide, MW=639g/mol, Genemed Synthesis, Inc., San Antonio, TX), an alternating cationic-aromatic peptide, are selective mitochondrial ROS inhibitors which significantly improved post-reperfused cardiac function compared to untreated I/R controls in this study ($p < 0.05$). MitoQ elicits antioxidant effects through the recycling of ubiquinone to ubiquinol, whereas SS-31 utilizes an antioxidant dimethyltyrosine residue. Improvement in post-reperfused cardiac function by MitoQ or SS-31 was associated with a significant decrease in myocardial tissue infarct size compared to untreated I/R hearts ($p < 0.01$). These results suggest mitochondrial-derived ROS are important contributors to I/R injury, and MitoQ or SS-31 when administered at reperfusion may potentially augment the benefits of angioplasty or

thrombolytic treatment in the clinical setting for myocardial infarction, where pretreatment may not be a practical option.

TABLE OF CONTENTS

List of Figures.....	vii
List of Tables.....	viii
Acknowledgments.....	ix
Introduction.....	1
Hypothesis.....	19
Methods.....	20
Results.....	25
Discussion.....	36
References.....	47

LIST OF FIGURES

Electron transport chain function in physiological conditions.....	5
Electron transport chain function at reperfusion.....	5
Schematic diagram of PKC-mediated ROS overproduction in I/R.....	8
Structure of the mitochondrial permeability transition pore.....	12
Mitochondrial permeability transition pore in apoptosis pathways.....	13
Reduction of mitochondrial ROS limits excess cell death.....	14
Isolated perfused rat heart image.....	20
Myocardial I/R protocol.....	21
Initial and final LVDP: I/R + MitoQ.....	26
Initial and final dP/dt_{max} : I/R + MitoQ.....	27
Initial and final dP/dt_{min} : I/R + MitoQ.....	27
Time course of LVDP: I/R + MitoQ.....	28
Time course of dP/dt_{max} : I/R + MitoQ.....	29
Time course of dP/dt_{min} : I/R + MitoQ.....	29
Initial and final LVDP: I/R + SS-31.....	30
Initial and final dP/dt_{max} : I/R + SS-31.....	31
Initial and final dP/dt_{min} : I/R + SS-31.....	31
Time course of LVDP: I/R + SS-31.....	32
Time course of dP/dt_{max} : I/R + SS-31.....	33
Time course of dP/dt_{min} : I/R + SS-31.....	34
Representative cross sections of I/R left ventricles stained for infarct size.....	34
Ratio of infarct size to total cardiac tissue at risk.....	35

LIST OF TABLES

Isolated Perfused Rat Heart Treatment Groups.....	23
Infarct Size and Cardiac Function Percent Recovery.....	25

ACKNOWLEDGMENTS

I would like to acknowledge the following people for their contributions to my thesis:

Dr. Lindon H. Young, Professor of Biomedical Sciences, Thesis Advisor

Dr. Robert Barsotti, Professor of Biomedical Sciences, Thesis Committee Member

Dr. Ruth Borghaei, Professor of Biomedical Sciences, Thesis Committee Member

Dr. Qian Chen, Research Assistant Professor of Biomedical Sciences

Dr. Marcus Bell, Director of Graduate Program in Biomedical Sciences

Christine Hammond, Laboratory Research Coordinator II

James Wood, Director of Laboratory Animal Resources

William Chau, Katelyn Navitsky, On Say Lau, Issachar Devine, Tyler Galbreath, Matthew Bertolet, Alexandra Lopez, Hung Pham; Philadelphia College of Osteopathic Medicine Students

Center for Chronic Disorders of Aging (C.C.D.A.)

The Department of Biomedical Sciences, Philadelphia College of Osteopathic Medicine

INTRODUCTION

The Clinical Setting of Myocardial I/R

Ischemic heart disease is the leading cause of morbidity and mortality in the industrialized world and also is the leading cause of mortality in the United States, accounting for nearly 20% of all deaths in the United States(1-5). Acute myocardial infarction can progress into persisting conditions of morbidity, such as heart failure(5, 6). During myocardial ischemia the coronary blood flow is interrupted, depriving cardiomyocytes of oxygen (O₂), glucose, and fatty acids. Ischemia lasting for 30 minutes or longer will result in irreversible cardiac damage(7). Quickly restoring blood flow (i.e., reperfusion) following ischemia is critical in salvaging heart tissue. Surgical interventions, such as coronary angioplasty or emergency coronary artery bypass grafting, as well as thrombolytic drug treatments can enable restoration of coronary blood flow to reduce the amount of irreversible tissue damage that occurs in the myocardium during periods of prolonged ischemia(5, 8). However, as coronary blood flow is reestablished, ischemic damage is exacerbated by a burst of reactive oxygen species (ROS) generated within seconds of reperfusion(8, 9). Increased oxidative stress during reperfusion contributes to the death of cardiomyocytes that were viable before reperfusion occurred(10, 11). It has been suggested that up to 50% of myocardial infarct size is due to reperfusion injury occurring after ischemia, and the prognosis for patients surviving an acute myocardial infarction is dependent on infarct size(5, 10). Clinical treatment of I/R injury remains a

challenge as no approved pharmaceutical agents effectively limit I/R-induced damage(4, 12).

The Need for Preclinical Investigation of Myocardial I/R

Jennings et al. first described the concept of myocardial I/R injury in 1960 using a canine I/R model, which resulted in cell swelling, myofibril contracture, sarcolemma disruption, and calcium phosphate accumulation within mitochondria(13). Treatment of myocardial I/R injury remains to be a challenge because reperfusion itself is associated with ventricular arrhythmias, stunning (i.e., contractile dysfunction of viable cells), and coronary vascular dysfunction(8, 10). Identifying the specific mechanisms by which myocardial I/R injury occurs will allow for the development of efficient treatment strategies to reduce I/R injury in myocardial infarction or heart transplantation patients and further prevent ischemic heart failure. Effective cardioprotective treatment should reduce both the amount of tissue infarction and viable cell dysfunction.

Implications of Mitochondria in Myocardial I/R

Ischemia has a direct effect on adenosine triphosphate (ATP) production. As previously mentioned, ischemia prevents cardiomyocytes from receiving O₂, glucose, and fatty acids and also reduces the amount of adenine nucleotides and cytochrome c available in mitochondria. Since mitochondria consume 85 to 90% of the O₂ in a cell to synthesize ATP from adenosine diphosphate (ADP) and inorganic phosphate (P_i) during oxidative phosphorylation, the function of

mitochondria is quickly disrupted by ischemia. Under normal conditions, mitochondria produce over 90% of cellular energy in the form of ATP. Ischemic conditions disrupt ATP production, leading to an overproduction of ROS at reperfusion with the reestablishment of O₂ supplied by coronary blood vessels. Mitochondria are implicated in I/R as a major source of ROS(14-20). Excess ROS leads to mitochondrial and cardiac contractile dysfunction, which can result in cell damage and additional tissue death, contributing to I/R injury.

Mitochondria, Both a Source and a Target for ROS

Mitochondria are extremely susceptible to oxidative damage since a large amount of ROS is generated within the mitochondria during I/R(14-18, 20). An excess of ROS leads to mitochondrial dysfunction, which is an important factor in the development of cardiac hypertrophy, contractile dysfunction, and subsequent heart failure(1, 6, 21). This sequence of events could lead to a decreased ability to recover from myocardial I/R and reduce the quality of life in patients following myocardial I/R. In dysfunctional myocardium, there is a significant increase in ROS production(1, 21, 22). Increased ROS production in dysfunctional mitochondria induces further ROS production resulting in a feed forward-loop of ROS elevation(14, 18). Dysfunctional mitochondria are associated with increased ROS production and oxidative mitochondrial DNA damage due to their inability to produce energy through the electron transport chain (ETC) complexes(6, 12, 21). Since mitochondrial DNA is situated closer to the primary site of ROS generation

and lacks both protective histones and efficient DNA repair mechanisms, it can easily become mutated and potentially lead to cardiomyopathy(14, 18, 23, 24).

**Sequence of ROS-Mediated I/R Damage:
The Mitochondrial Respiratory Chain Releases ROS**

Oxidative phosphorylation is inactivated by ischemia, which results in an accumulation of phosphate, fatty acids, lactic acid, and cellular calcium while decreasing cellular pH and the amount of adenine nucleotides and cytochrome *c* available in the mitochondria(10, 12, 25, 26). The rapid restoration of the decreased pH upon reperfusion, possibly involving the opening of the mitochondrial permeability transition pore complex (MPTP), is a contributing factor to I/R injury. Reoxygenation with an acidic buffer inhibits opening of the MPTP(10, 27). At the time of reperfusion, a burst of ROS including superoxide (SO), hydrogen peroxide (H_2O_2), and peroxynitrite are generated by the interaction of O_2 with the damaged mitochondrial respiratory chain, primarily through the uncoupling of complexes I and III(12, 28, 29). It is suggested that a large portion of ROS in the I/R heart is a result of the uncoupling of complexes I and III in the mitochondrial ETC(28). Under physiological conditions O_2 is the final electron acceptor, accepting four electrons from complex IV, and is used to produce water (H_2O), a by-product of respiration(14, 18)(Figure 1).

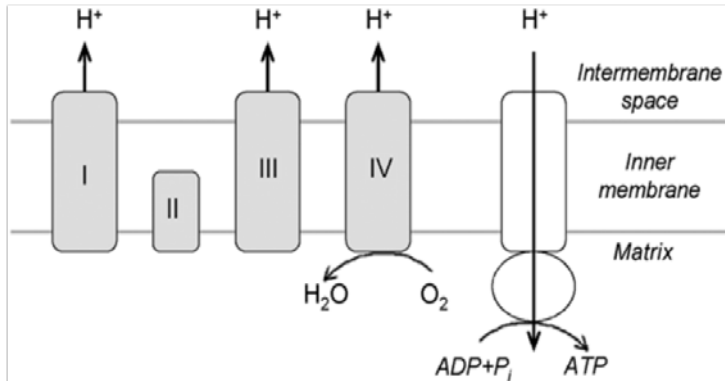


Figure 1. Electron transport chain (ETC) function in physiological conditions. Maintenance of the electrochemical gradient of the mitochondrial membranes by the ETC is essential for ATP production. In these conditions, oxygen (O_2) accepts four electrons from complex IV. Adapted from Szeto 2006.

However, in dysfunctional mitochondria, electrons leaking from complexes I and III are accepted by O_2 to generate SO , a form of ROS(14, 18, 30)(Figure 2).

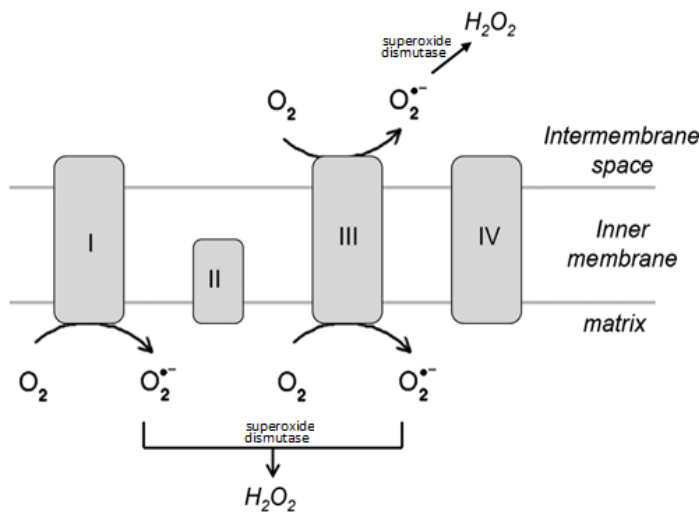


Figure 2. Electron transport chain (ETC) function at reperfusion. Oxygen (O_2) generates superoxide (O_2^-) by accepting electrons leaking from complexes I and III. Even though O_2^- cannot diffuse across membranes, O_2^- is generated in both the intermembrane space and within the matrix by this mechanism. Forms of superoxide dismutase can quickly convert O_2^- to hydrogen peroxide (H_2O_2), which is more stable and able to diffuse into the cytosol. Adapted from Szeto 2006 and modified.

Excessive amounts of ROS produced during myocardial I/R overwhelm the physiological antioxidant mechanisms of glutathione, glutathione peroxidase, thioredoxin, glutaredoxin-tocopherol, ubiquinol, ascorbic acid, superoxide dismutase, and catalase(14, 18, 21, 26). The release of excess ROS damages cells directly. As a signaling molecule, ROS can activate hypertrophy and apoptosis pathways(21, 31-33). ROS directly damages nucleic acids, proteins,

and lipids, consequently disrupting membrane integrity and cell function as a result(14, 18, 21, 26, 30). SO can quickly be converted into H_2O_2 , which is more stable, has a longer half-life, and can diffuse across the mitochondrial membranes into the cytosol(14, 32, 34). Conversion of H_2O_2 into hydroxyl radicals or carbonate anions, which are both highly reactive forms of ROS, can further promote oxidative stress(14). Adult rat cardiomyocytes treated with H_2O_2 showed that H_2O_2 concentration-dependently activates four kinase signaling pathways (i.e., ERK1/2, p38 kinase, JNK, and Akt) involved in the regulation of cardiomyocyte hypertrophy and/or apoptosis. Lower H_2O_2 concentrations resulted in hypertrophy, while higher H_2O_2 concentrations induced apoptosis(31, 35, 36). Varying levels of oxidative stress induced in neonatal rat ventricular myocytes also showed the same concentration-dependent effect of ROS on cardiac hypertrophy and apoptosis(32, 37-40). Nitric oxide (NO) can interact with SO to form peroxynitrite, a highly reactive form of ROS(30, 41). Peroxynitrite can rapidly modify proteins, DNA, and membranes to cause oxidative damage(10, 21, 30, 42) and irreversibly inhibit cellular respiration(43).

Sequence of ROS-Mediated I/R Damage: NADPH Oxidase, Another Important ROS Source

Another source of ROS that originates in the mitochondria of cardiomyocytes and endothelial cells is nicotinamide adenine dinucleotide phosphate oxidase (Nox)(10, 22, 44-48). Nox4, for example, is primarily localized in mitochondria and exhibits increased ROS producing activity in dysfunctional cardiomyocytes(22, 44-48). Genetic deletion of p47^{phox}, the cytosolic component

of Nox, has confirmed the implication of Nox in ROS-induced cardiac dysfunction in a mouse myocardial infarction model. Analysis 30 days following myocardial infarction showed that there was a reduction in left ventricular remodeling, dysfunction, and dilation which paralleled the decrease in cardiomyocyte apoptosis, hypertrophy, and interstitial fibrosis at the same time point. These results also suggest that Nox may be involved in the development of heart failure following myocardial infarction(6, 28, 48). However, it has been suggested that Nox4, which is primarily localized in mitochondria, does not require p47phox, p67phox, or Rac for activation but is dependent on SO levels for its expression. At both cardiac cellular and tissue levels, the overexpression of Nox4 has been shown to increase SO generation in mitochondria and contribute to cardiac dysfunction, fibrosis, apoptosis, and mitochondrial dysfunction(49).

Sequence of ROS-Mediated I/R Damage: ROS-induced eNOS Uncoupling

The production of ROS during reperfusion from mitochondria and Nox can stimulate further increases in ROS formation as a feed-forward loop. ROS from these sources may oxidize tetrahydrobiopterin (BH₄) to dihydrobiopterin (BH₂) and consequently promote eNOS uncoupling, which leads to additional ROS production(29, 50). When using BH₂ as a co-factor, endothelial nitric oxide synthase (eNOS) is considered uncoupled and produces SO instead of NO. The release of SO from uncoupled eNOS causes oxidative damage and increases production of other forms of ROS(51). A schematic diagram of the implications of uncoupled eNOS in continuing the feed-forward loop of excessive ROS

production in I/R is shown in Figure 3. This diagram focuses on protein kinase C (PKC)-mediated ROS generation in I/R as an example, though other pathways contributing to the feed-forward loop of ROS overproduction in I/R exist.

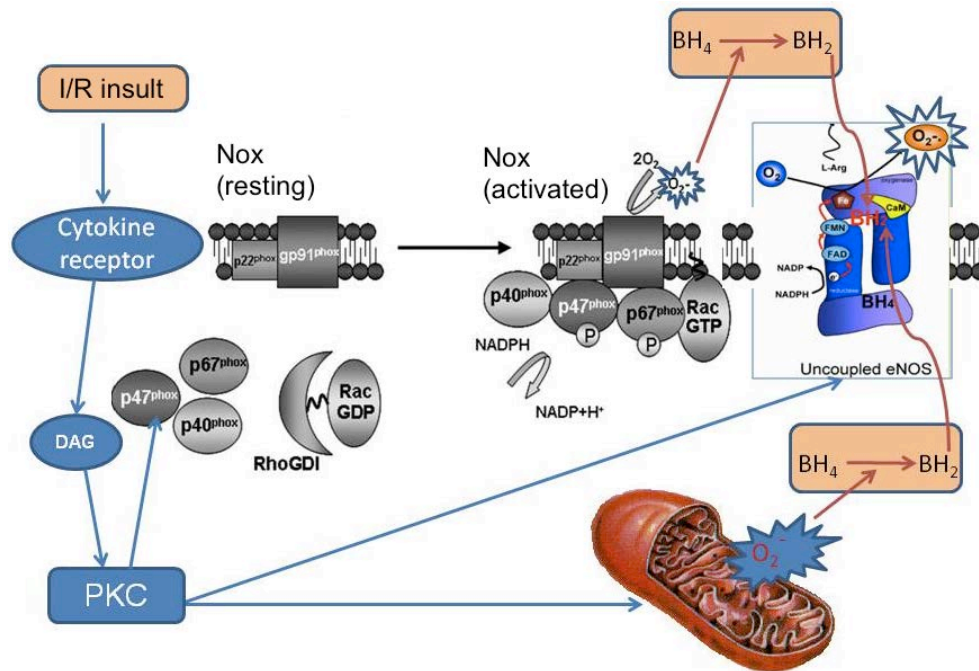


Figure 3. Schematic diagram of protein kinase C (PKC)-mediated ROS overproduction in ischemia/reperfusion (I/R). The insult caused by I/R stimulates the release of cytokines, which activate cytokine receptors. These cytokine receptors in turn generate diacylglycerol (DAG), a second messenger signaling lipid which activates PKC. PKC phosphorylates p47phox, an essential component in NADPH oxidase (Nox) activity, to activate Nox, resulting in SO (O_2^-) release. Phosphorylation by PKC can also directly promote O_2^- release from mitochondria and uncoupled eNOS. All of these sources of excess O_2^- contribute to the oxidation of BH₄ to BH₂, which promotes further eNOS uncoupling, resulting in a feed-forward loop of ROS overproduction during I/R. Adapted and modified from Schmidt and Alp 2007.

It has previously been shown that eNOS uncoupling is a major source of ROS in a hind limb I/R model and contributes to post-reperused cardiac contractile dysfunction in myocardial I/R(52). The uncoupling of eNOS can quickly cause endothelial dysfunction within the first 5-10 min of reperfusion(52, 53). Hemodynamic stress is also known to lead to eNOS uncoupling. However, supplementation with BH₄ in mice with heart disease following pressure overload

prevents eNOS uncoupling and reduces left ventricular hypertrophy, cardiac dysfunction, and fibrosis (54). Folic acid also restores reduced BH₄ production, which increases coupled eNOS activity to protect the heart. Folic acid preserves cardiac function in I/R rats, suggesting that there is a cardioprotective effect in decreasing ROS production by increasing available BH₄ to increase coupled eNOS activity in I/R(55). Coupled eNOS produces NO.

Once NO is released it acts as a diffusible signaling molecule and regulates blood pressure by increasing the production of cyclic guanosine monophosphate (cGMP) to relax smooth muscle(1). Previous studies have shown that the pathway between eNOS, NO, and cGMP is an essential activator of mitochondrial biogenesis(56, 57). Mitochondrial biogenesis increases energy production and has a cardioprotective function in studies using rats, dogs, and humans(58-62). NO is able to improve coronary blood flow, inhibit accumulation of neutrophils, and inactivate SO radicals(10, 43, 63). The importance of these effects of NO were demonstrated by systemically inhibiting NO synthesis *in vivo*, resulting in peripheral vasoconstriction and hypertension, which induce cardiovascular reflexes that change preload, afterload, and heart rate(43, 64, 65). Additionally, it has been shown that NO regulates cellular respiration in the myocardium by increasing the efficiency of O₂ consumption in oxidative phosphorylation. Inhibiting NO synthesis at all levels of cardiac contractile performance significantly increased O₂ consumption with no effect on the rate of ATP synthesis or amount of ATP produced, suggesting that the effect of inhibition of NO synthesis is unrelated to contractile performance. It has therefore

been suggested that endogenous NO enhances the coupling of O₂ consumption to both ATP synthesis and cardiac performance(43). Despite its cardioprotective effects, NO is also known to reversibly bind to cytochrome *c* to inhibit energy production in the mitochondria and produce ROS and reactive nitrogen species by displacing O₂(66). NO can react with SO to generate peroxynitrite, a highly reactive form of ROS(30, 42). NO is also able to induce apoptosis by activating the opening of the MPTP(41). It has been demonstrated that at pathological concentrations, NO activity switches from an anti-apoptotic effect to a pro-apoptotic effect(67, 68) Endothelial dysfunction is a key event to induce leukocyte mediated inflammation leading to contractile dysfunction in the myocardium(52, 53). This sequence of events contributes to I/R injury. However, initiating sources of ROS that induce eNOS uncoupling are not well defined. Investigating the initiating sources of ROS and ways to inhibit excess ROS production in I/R is therefore of great significance.

Sequence of ROS-Mediated I/R Damage: Lipid Peroxidation and Mitochondrial Permeability

As mentioned before, excess release of ROS leads to an increased production of ROS. Lipid peroxidation can occur as a result of ROS release during I/R and cause membrane damage, such as loss of membrane potential. Lipid peroxidation can damage the sarcolemmal membrane and cause an increase of intracellular calcium that overwhelms the physiological calcium regulation mechanisms(10-12, 26). Excessive increases in intracellular calcium leads to cardiac hypertrophy, fibrosis, opening of the MPTP, contractile

dysfunction, cell death, and potentially heart failure(10, 11, 69). The opening of the MPTP induces cell death by the irreversible loss of the mitochondrial electrochemical membrane, causing mitochondrial swelling and rupture. Cytochrome *c* release from the MPTP into the cytosol inhibits electron transport and activates caspase mediated apoptosis cascades(12, 69, 70). Linoleic and arachidonic acid, for example, are unsaturated fatty acids that create 4-hydroxynonenal (HNE) as a by-product of their peroxidation. HNE can create protein adducts and cause additional lipid peroxidation. HNE also induces formation of mitochondrial membrane permeabilization (MMP) and subsequent apoptosis. NO, peroxynitrite, and HNE can each independently cause lipid peroxidation and MMP. It is suggested that this effect is mediated by MPTP since the opening of the pore by this mechanism is inhibited by cyclosporin A, a direct inhibitor of the MPTP(71). Cyclosporin A binds to cyclophilin D and detaches cyclophilin D from the inner mitochondrial membrane(72) (Figure 4). The MPTP is a channel made up of proteins that form a complex to span the inner and outer mitochondrial membranes. The adenine nucleotide translocator, cyclophilin D, and the voltage-dependent anion channel are the key functional MPTP constituents(18, 72)(Figure 4).

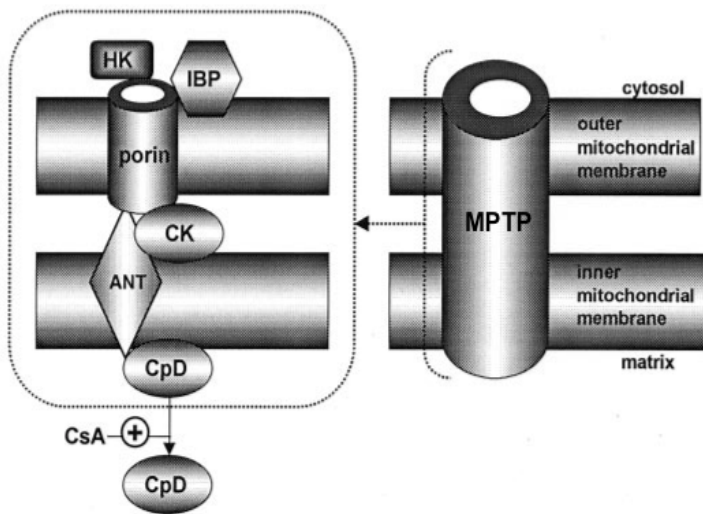


Figure 4. The mitochondrial transition pore (MPTP) spans the outer and inner mitochondrial membranes. The peripheral benzodiazepine receptor (IBP), hexokinase (HK), adenine nucleotide translocase (ANT), creatine kinase (CK, in muscle mitochondria) and cyclophilin D (CpD) are the basic subunits of the MPTP. When cyclosporin A (CsA) binds (\oplus) to CpD, CpD is unable to associate with the MPTP, preventing the MPTP from opening. Adapted and modified from Szewczyk and Wojtzak 2002.

Although the mechanism by which NO, peroxynitrite, and HNE initiate MMP has not been clearly defined, the adenine nucleotide translocator component of the MPTP responds to these forms of ROS by opening the MPTP to increase MMP. MMP can affect both the outer and inner mitochondrial membranes simultaneously, or each individually. The opening of the MPTP uncouples oxidative phosphorylation, reducing the amount of ATP available, and allows the release of compounds normally sequestered by either or both of the mitochondrial membranes(10, 42, 69). Both of these effects can result in cell death. For example, prolonged MPTP opening can cause a loss of electrochemical membrane potential and release cytochrome *c*, Smac/DIABLO, and apoptosis-inducing factor (AIF) from the intermembrane space to activate apoptosis pathways, including those mediated by caspase activity(26, 41)(Figure 5).

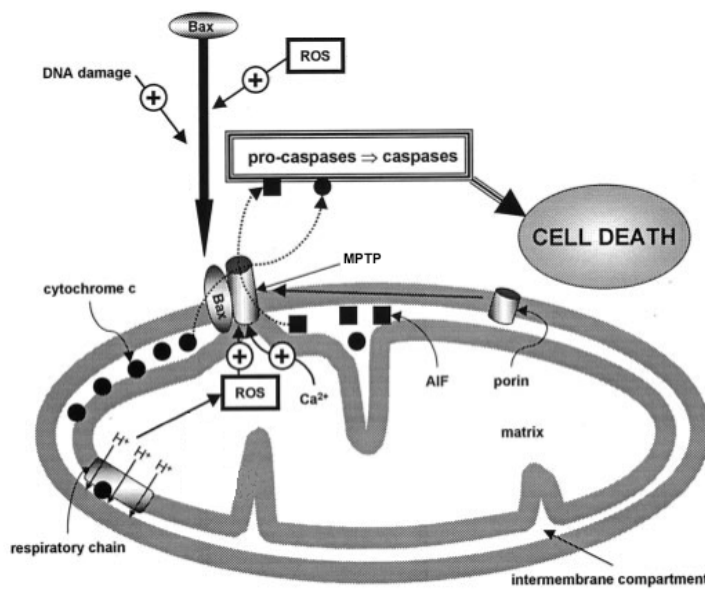


Figure 5. The mitochondrial transition pore (MPTP) in apoptosis pathways. ROS, DNA damage, and other apoptosis-inducing signals promote the binding of Bax, a proapoptotic protein, with the outer mitochondrial membrane near the MPTP. Bax activity promotes the opening of the MPTP, which releases cytochrome c and apoptosis-inducing factor (AIF) into the cytosol. Elevated calcium and ROS can also directly stimulate MPTP opening. The release of cytochrome c and AIF into the cytosol activates caspase-mediated apoptosis pathways. Adapted from Szewczyk and Wojtzak 2002 and modified.

Mitochondria as a Potential Therapeutic Target in I/R

Although mitochondrial-targeted antioxidant pretreatment can effectively limit I/R injury, pretreatment is not always possible in cases of myocardial infarction(5, 15, 16, 73, 74). Therefore, evaluating the cardioprotective efficacy of mitochondrial-targeted antioxidants when given at reperfusion is of high significance. Previous studies have shown that selective mitochondrial antioxidants administered before ischemia and at reperfusion can reduce heart, liver, and kidney damage beginning immediately following ischemia, thus suggesting that selective mitochondrial antioxidants can work quickly in attenuating I/R injury(18, 30, 75). If these agents can work expeditiously and effectively when administered at the time of coronary blood flow restoration, mitochondrial-targeted antioxidants may be a practical option in the clinical

setting in cases of myocardial infarction. Following myocardial I/R, treatments that can attenuate endothelial and cardiac contractile dysfunction will limit tissue damage and allow these patients to have a better quality of life.

Mitoquinone, a Mitochondrial-Targeted Antioxidant

Conventional antioxidants, such as coenzyme Q, vitamin E, and N-acetylcysteine, have limited efficacy in protecting mitochondria from oxidative damage because they are not targeted selectively to the mitochondria, where most I/R damage occurs(14-18, 26). Therefore, selectively targeting mitochondria with antioxidants may be an effective strategy to attenuate release of mitochondrial ROS (Figure 6).

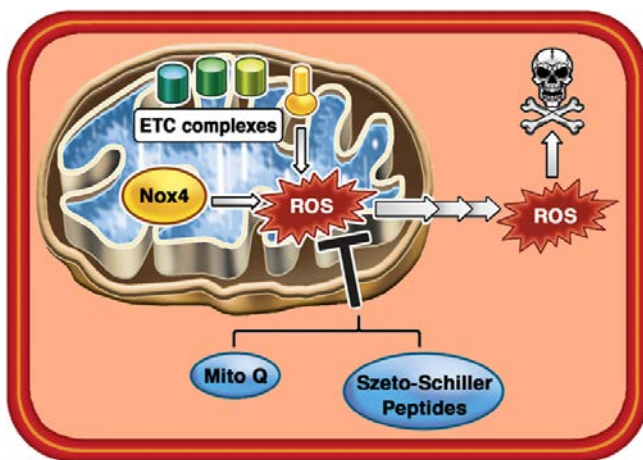


Figure 6. Reduction of mitochondrial reactive oxygen species (ROS) limits excess cell death. Mitochondrial ROS stimulate ROS production outside mitochondria, increasing oxidative stress and apoptosis signaling cascade activation. ETC complexes and Nox4 are major ROS sources in dysfunctional mitochondria. Specific mitochondrial-targeted antioxidants exert cardioprotective effects. Adapted from Bayeva et al. 2013 and modified.

Attachment of an antioxidant to a lipophilic cation allows the antioxidant to concentrate 100 to 1000-fold within mitochondria(14, 17, 76). Mitoquinone (MitoQ, MW=579g/mol; the MitoQ referred to in this study was complexed with cyclodextrin (MW=1135g/mol) to improve water solubility, total MW=1714g/mol), a coenzyme Q analog, incorporates a lipophilic triphenylphosphonium (TPP)

cation, which easily passes through phospholipid bilayers and is driven by the large electrochemical mitochondrial membrane potential (150-180 mV), to concentrate MitoQ specifically within the mitochondria at a several hundred-fold concentration(16-18, 76). The TPP cation is covalently attached to an ubiquinol antioxidant to scavenge ROS and prevent lipid peroxidation(1, 16, 17, 76, 77). After entering the mitochondria, the respiratory chain reduces MitoQ to its active ubiquinol form. A previous study has shown that accumulation of ubiquinol within mitochondria is necessary for the efficacy of MitoQ in limiting myocardial I/R injury since quinol by itself is unable to cross the mitochondrial membrane(16). The oxidation of MitoQ into its quinone form scavenges ROS inside mitochondria; complex II of the respiratory chain then recycles MitoQ back into its active quinol form continuously after each time MitoQ completes antioxidant activity(16, 17, 78). Another aspect of MitoQ that could make it an attractive therapeutic tool is that no significant adverse effects have been reported after long-term administration. MitoQ does not act as a pro-oxidant in wild-type mice in vivo(17). No significant adverse effects were reported when MitoQ was administered as an oral tablet to patients for up to a year, however there was mild nausea and vomiting reported in the MitoQ treatment groups(76, 79). In one study, administration of MitoQ (500 μ M in drinking water) to mice for 20-28 weeks allowed MitoQ to accumulate primarily in the liver and heart but also slightly in the brain. Long term MitoQ administration did not increase mitochondrial oxidative stress in vivo, suggesting that MitoQ does not have pro-oxidant effects when administered over an extended period of time. Additionally, mitochondrial

enzyme activity was not negatively affected. MitoQ seemed to reduce plasma levels of triglyceride but did not alter glucose, insulin, free fatty acid, or cholesterol levels in plasma. Additionally, these MitoQ treated mouse heart and liver tissues did not have any significant differences in their gene expression profile compared to untreated controls(17). In human studies where MitoQ was administered orally as a daily dose for up to one year, no severe side effects were reported(76, 79). Another aspect of TPP conjugated antioxidants is that uptake is reversible; they can be rapidly cleared from any organ of the body once administration is stopped(80).

SS-31, Also a Mitochondrial-Targeted Antioxidant

The SS-31 (Szeto-Schiller) peptide ((D-Arg)-Dmt-Lys-Phe-Amide, MW=639 g/mol, Genemed Synthesis, Inc., San Antonio, TX) is also of interest in further understanding the role of mitochondrial derived ROS and efficacy of inhibiting mitochondrial ROS production in myocardial I/R. SS-31 is a cell-permeable peptide, specifically targeted to inner mitochondrial membranes based on its alternating aromatic residues and basic amino acid sequence, with an antioxidant dimethyltyrosine moiety (Dmt)(14, 26). Tyrosine scavenges ROS to form unreactive compounds, attributing the ability of SS-31 to scavenge ROS to the Dmt amino acid residue, which has been found to be more effective than tyrosine(18, 81, 82). The backbones of most peptides have a tendency to form hydrogen bonds with water, making these peptides not cell-permeable. However, the alternating aromatic-cationic motif of SS-31 allows it to rapidly diffuse through

cell membranes(18). Unlike TPP-conjugated antioxidants, SS-31 does not rely on the electrochemical mitochondrial membrane potential to selectively accumulate 10,000-fold inside mitochondria(14, 18). In dysfunctional mitochondria, the electrochemical membrane potential may be disrupted(18, 73). Therefore, the ability to target an antioxidant selectively to mitochondria independent of membrane potential may prove useful in I/R. Additionally, high doses of lipophilic cation attached antioxidants may depolarize the mitochondrial membrane potential, but SS-31 at concentrations as high as 1 mM did not depolarize the mitochondrial membrane potential(14, 18, 26). SS-31 can cross plasma membranes in both directions in an energy-independent manner(14, 26, 83). In liver and brain mitochondria, SS-31 reached its maximum intracellular concentration within 2 min of incubation(26). SS-31 achieved steady state by 30 minutes of incubation with neuronal cell lines(26). SS peptides have relatively long elimination half-lives and are also small, water soluble, stable and resistant to peptidase degradation(14, 26). When SS-31 was incubated in mouse, rat, dog, monkey and human plasma at 37 °C for 1 hour there was little degradation. SS-31 was most stable in human plasma, with a half-life of about 30 hours, and was classified as a low clearance compound in human liver microsomes(12, 84). Previous studies have shown that in *ex vivo* and *in vivo* I/R models, SS peptides scavenge H₂O₂, hydroxyl radicals, and peroxynitrite while also inhibiting lipid peroxidation. Consequently, there is less cytochrome c release and subsequent oxidant-induced cell death because the opening of the MPTP is inhibited(12, 14, 18, 26, 73, 85). Since SS-31 reduced infarct size and tissue dysfunction in I/R

models as a pretreatment, it is possible that SS-31 would have a similar effect when administered at reperfusion(86). One limitation of previous studies is that they did not measure both cardiac function and infarct size in the same animals that were administered SS-31 exclusively at the time of reperfusion.

HYPOTHESIS

It has previously been determined that the formation of ROS within the mitochondria under I/R conditions is a major contributor to I/R injury(14-16). It is hypothesized that antioxidants specifically targeted to the mitochondria to attenuate ROS formation will reduce I/R injury by limiting cardiac contractile dysfunction and cardiac tissue damage. MitoQ, a coenzyme Q derivative, and SS-31, an alternating cationic-aromatic peptide, are selective mitochondrial ROS inhibitors. MitoQ incorporates a lipophilic TPP cation covalently attached to a ubiquinol antioxidant, whereas SS-31 is a cell-permeable peptide with an antioxidant dimethyltyrosine residue specifically targeted to the inner mitochondrial membrane based on its alternating cationic aromatic residue sequence(15, 16, 87). It is expected that the myocardial I/R rat hearts treated with MitoQ or SS-31, given at reperfusion, will have greater preserved cardiac contractile function and smaller infarct size following myocardial I/R in comparison to the untreated I/R rat hearts.

METHODS

Isolated Rat Heart Preparation

Male Sprague-Dawley rats (275-325 g, Charles River, Springfield, MA) were anesthetized intraperitoneally (i.p.) with pentobarbital sodium (60 mg/kg); the injection also contained sodium heparin (1,000 U). Each heart was rapidly excised and subjected to retrograde perfusion via the aorta with a modified Krebs-Henseleit buffer (in mmol/L: 17.0 dextrose, 120.0 NaCl, 25.0 NaHCO₃, 2.5 CaCl₂, 0.5 EDTA, 5.9 KCl and 1.2 MgCl₂). The perfusate was maintained at 37 °C, kept at 80 mmHg constant pressure, aerated with 95% O₂-5% CO₂ and equilibrated at a pH of 7.35-7.45(88, 89).

The aorta of the isolated rat heart was cannulated onto a perfusion needle and immersed in a water-jacketed reservoir containing 160 mL of modified Krebs-Henseleit buffer (Figure 7).



Figure 7. The isolated perfused rat heart was cannulated via the aorta with a perfusion needle while immersed in a water-jacketed reservoir containing 160 mL of modified Krebs-Henseleit buffer. Also shown in this picture is the pressure transducer inserted into the left ventricular cavity to monitor cardiac function parameters.

A flowmeter (T106, Transonic Systems, Inc., Ithaca, NY) was inserted into the perfusion line to monitor coronary flow. Left ventricular end-systolic pressure (LVESP), left ventricular end-

diastolic pressure (LVEDP), heart rate, and the peak rates of rise and fall in the

first derivative of left ventricular pressure (dP/dt_{\max} and dP/dt_{\min} , respectively) were monitored using a pressure transducer (SPR-524, Millar Instruments, Inc., Houston, TX) positioned in the left ventricular cavity and recorded using a Powerlab Station acquisition system (ADInstruments, Grand Junction, CO). Left ventricular developed pressure (LVDP) was calculated by subtracting the LVEDP from the LVESP. Insertion of the pressure transducer catheter into the left ventricle allowed Krebs' buffer to fill the left ventricle and establish preload volume. During the baseline period, the preload of the hearts of all study groups were be similar due to the limited weight range (275-325 g) of the animals as seen in previous studies(89-91). The initial baseline LVEDP was between 4-9 mmHg for all hearts in each study group. Coronary flow, LVESP, LVEDP, heart rate, dP/dt_{\max} , and dP/dt_{\min} were measured every 5 min for 15 min to ensure that stable baseline measurements were obtained. Figure 8 illustrates a schematic diagram of the I/R protocol in the isolated perfused rat heart.

baseline stabilization 15 min	ischemia 30 min	reperfusion 45 min	TTC staining
↑ heart connected to I/R apparatus	↑ flow of modified Krebs-Henseleit buffer reduced to 0	↑ autologous plasma ± MitoQ or SS-31 infusion	

Figure 8. Myocardial I/R protocol. A 30 min perfusion period replaced ischemia in sham groups. At the beginning of the 45 min reperfusion period, 5 mL of autologous plasma ± MitoQ or SS-31 was infused 1 mL/min for 5 min.

Once a stable baseline was established, ischemia was induced for 30 min by quickly reducing the flow of Krebs' buffer to zero. One of the three side arms in the perfusion line proximal to the heart inflow cannula was used for the infusion of 5 mL of autologous plasma (control hearts) or autologous plasma

containing MitoQ (1, 10, 20 μ M) or SS-31 (25, 50, 100 μ M). After 30 min of ischemia, the flow of Krebs' buffer was restored simultaneously with an infusion of either 5 mL of plasma (control I/R) or 5 mL of plasma containing MitoQ or SS-31 at a rate of 1 mL/min for 5 min. Sham hearts were not subjected to ischemia and were given the 5 mL infusion of plasma at a rate of 1 mL/min for 5 min following 30 minutes of continuous perfusion in lieu of ischemia. Beginning at the infusion of plasma, cardiac function parameters were recorded every 5 min for 45 min.

At the end of the experimental protocol, the right and left ventricles were separated from each heart. Three sections of the left ventricle were used for 2,3,5- triphenyltetrazolium chloride (TTC) staining.

Groups of Isolated Perfused Hearts

The 9 groups of isolated perfused rat hearts used in the study are shown in Table 1. Two types of control groups were used in the study based on previously established myocardial I/R models. Sham hearts were continuously perfused with the modified Krebs-Henseleit buffer for a 30 min period in lieu of the 30 min ischemia period and infused with 5 mL of plasma (1 mL/min) immediately following the 30 min perfusion period (i.e., the same time point that all I/R hearts would be given 5 mL of plasma). This group was utilized to show that cardiac function (i.e., LVDP, dP/dt_{max} , dP/dt_{min} , coronary flow,, and heart rate) is maintained with no significant changes over a 90 min isolated perfused heart protocol, suggesting that any damage or cardiac dysfunction is due to injury

associated with ischemia and reperfusion. Control I/R hearts were subjected to a 30 min period of ischemia followed by 45 min of reperfusion including an infusion of 5 mL of plasma (1 mL/min) in the first 5 min of reperfusion immediately following ischemia. This group was used to show the compromised postreperfused heart function after 30 min ischemia and 45 min reperfusion in the absence of any drugs compared to the baseline measurements of cardiac function. The drug treated I/R groups consist of I/R + MitoQ and I/R + SS-31 as shown in Table 1.

Table 1. Isolated Perfused Rat Heart Treatment Groups

		Control I/R	MitoQ			SS-31		
			1 μ M	10 μ M	20 μ M	25 μ M	50 μ M	100 μ M
<i>Sham</i>	n=6							
<i>I/R</i>	n=14	n=6	n=7	n=6	n=6	n=6	n=6	n=6

Isolation of Plasma

Blood was collected in 1 mL of citrate phosphate dextrose buffer (Sigma Chemical Co., St. Louis, MO) from the abdominal aorta of the same rat from which the heart was isolated for each myocardial I/R experiment to simulate *in vivo* conditions. The blood was centrifuged at 10,000 x g for 10 min at 4 °C. The plasma was decanted from the blood, and 5 mL of the plasma collected from each rat was used for its corresponding isolated perfused heart during the infusion period at the beginning of reperfusion in all myocardial I/R groups.

TTC Staining

Once the 45 min reperfusion period was complete, the right ventricle was separated from the left ventricle and placed in liquid nitrogen. The apex and two

middle sections were isolated from the base of the left ventricle, and the base of the left ventricle was placed in liquid nitrogen. The apex and two middle sections were each placed in 1 mL of TTC for 15 min to visualize infarcted tissue areas. TTC is a salt that can be reduced by dehydrogenases to triphenylformazan, a fat soluble, light-sensitive compound which stains viable tissue bright red. Areas deficient in dehydrogenase activity remain the pale white color of the TTC salt. Previous studies have shown that the differentiation between viable and infarcted tissue by TTC staining correlates with loss of dehydrogenase activity and is therefore a reliable tool to measure infarct size(92-94). The weight ratio of infarcted cardiac tissue to the total area of tissue at risk was calculated and statistically analyzed.

Statistical Analysis

All data in the text and figures were presented as means \pm SEM. The cardiac function and TTC staining data were analyzed by ANOVA using post hoc analysis with the Student-Newman-Keuls test. Probability values of <0.05 were considered to be statistically significant.

RESULTS

I/R + MitoQ (1 μ M, 10 μ M, 20 μ M)

Cardiac Function

Sham hearts, which were not subjected to ischemia, are shown in all cardiac function graphs as reference points to illustrate the impact of I/R on cardiac function. Table 2 expresses the percent recovery, a comparison of the final to initial values, and Figures 9, 10, and 11 show the initial and final values of LVDP, dP/dt_{max} , and dP/dt_{min} from each experimental group, respectively.

Table 2. Infarct Size (%) and LVDP, dP/dt_{max} , and dP/dt_{min} Percent Recovery

	Control I/R	MitoQ			SS-31		
		1 μ M	10 μ M	20 μ M	25 μ M	50 μ M	100 μ M
<i>Infarct Size</i>	45.0 \pm 2.1	53.9 \pm 6.3	26.7 \pm 3.2**	23.3 \pm 2.1**	25.2 \pm 3.8**	18.9 \pm 2.0**	20.6 \pm 1.9**
<i>LVDP</i>	47.6 \pm 3.0	58.9 \pm 9.2	76.7 \pm 4.0*	69.5 \pm 7.8*	47.3 \pm 5.9	80.6 \pm 3.4**	62.1 \pm 6.4
<i>dP/dt_{max}</i>	37.7 \pm 3.0	40.9 \pm 7.4	62.0 \pm 3.3*	55.2 \pm 5.4*	42.6 \pm 3.1	70.5 \pm 5.8**	49.0 \pm 2.6
<i>dP/dt_{min}</i>	48.7 \pm 1.3	59.4 \pm 8.8	72.1 \pm 8.2	63.5 \pm 10.4	43.1 \pm 5.2	81.4 \pm 4.1*	61.7 \pm 7.9

All data were analyzed using ANOVA with the Student Newman Keuls test (p <0.05, ** p <0.01 compared to control I/R)*

There was no statistically significant difference initially between the baseline values between any of the experimental groups. Additionally, there was no statistically significant difference between the initial and final values of LVDP, dP/dt_{max} , or dP/dt_{min} in the sham hearts. The sham hearts showed that there is not a significant decrease in cardiac function due to the experimental protocol in lieu of ischemia. In contrast, cardiac function of the control I/R hearts was significantly compromised by 45 min postreperfusion compared to baseline

cardiac function ($P < 0.01$). At the end of each experiment, control I/R hearts recovered to 47.6 ± 3.0 % of initial LVDP, 37.7 ± 3.0 % of initial dP/dt_{max} , and 48.7 ± 1.3 % dP/dt_{min} (Table 2, Figs. 9-11). I/R hearts treated with MitoQ (10, 20 μ M) significantly recovered in LVDP and dP/dt_{max} ($P < 0.05$ compared to control I/R; Table 2, Figs. 9 and 10); whereas lower dose (1 μ M) MitoQ was not statistically different from the I/R control (Table 2, Figs. 9 and 10). Interestingly, even though MitoQ (10, 20 μ M) was able to improve postreperfused dP/dt_{max} , there was not a significant difference in the postreperfused dP/dt_{min} between the MitoQ (10, 20 μ M) treated I/R hearts and untreated I/R hearts (Table 2, Fig. 11). Overall, these results suggest that the infusion of MitoQ (10, 20 μ M) at reperfusion improves postreperfused cardiac contractile function compared to I/R control hearts ($P < 0.05$).

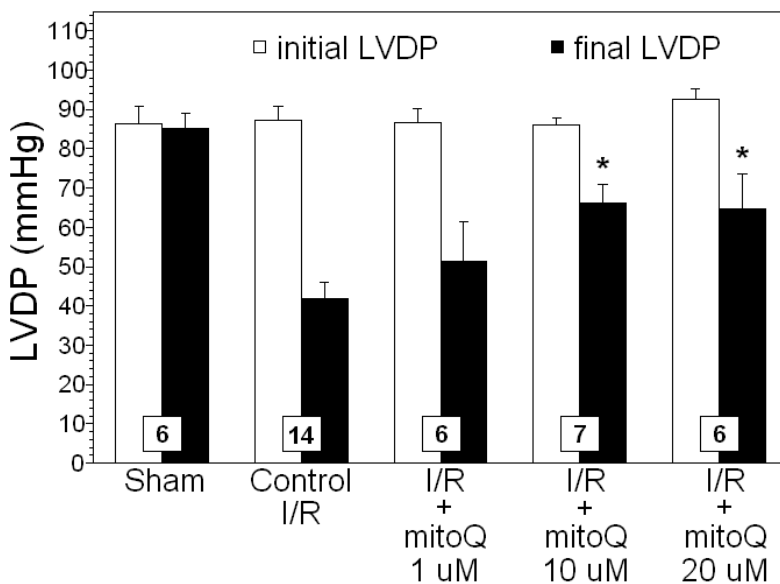


Figure 9. Initial (before ischemia) and final (at 45 min reperfusion) measurements from isolated perfused rat hearts of left ventricular developed pressure (LVDP), expressed in mmHg. (* $P < 0.05$ compared to control). All values are expressed as mean \pm SEM. The number of hearts in each experimental group is shown in the box at the base of each bar.

Figure 10. Initial (before ischemia) and final (at 45 min reperfusion) measurements from isolated perfused rat hearts of the peak rate of rise in the first derivative of left ventricular systolic pressure (dP/dt_{max}), expressed in mmHg/s. (* $P < 0.05$ compared to control). All values are expressed as mean \pm SEM. The number of hearts in each experimental group is shown in the box at the base of each bar.

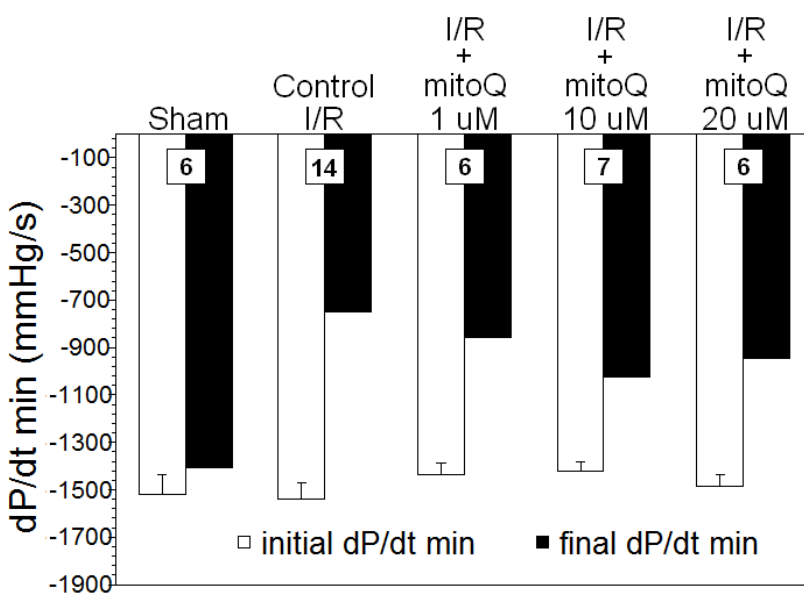
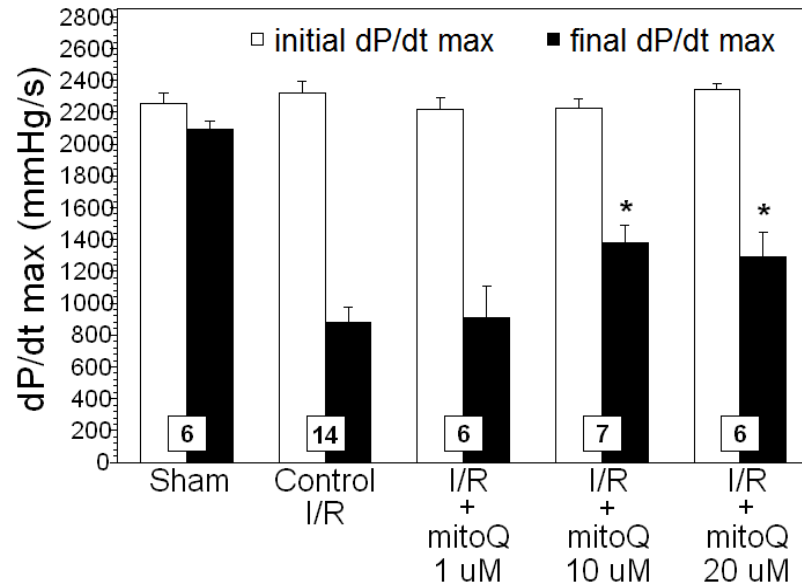


Figure 11. Initial (before ischemia) and final (at 45 min reperfusion) measurements from isolated perfused rat hearts of the minimal rate of left ventricular systolic pressure in the first derivative (dP/dt_{min}), expressed in mmHg/s. (* $P < 0.05$ compared to control). All values are expressed as mean \pm SEM. The number of hearts in each experimental group is shown in the box at the base of each bar.

Moreover, the time courses of LVDP, dP/dt_{max} , and dP/dt_{min} show that the I/R control group exhibited sustained contractile dysfunction throughout the 45 min period of reperfusion following ischemia compared to the sham hearts that did not experience ischemia ($P < 0.01$). However, the I/R hearts treated with 10 μ M MitoQ showed significantly recovered LVDP by the 20 min time point and

significantly recovered dP/dt_{max} by the 30 min time point, suggesting that cardiac contractile function can recover more quickly after an infusion of MitoQ (10 μ M) and sustain better contractile function by 45 min of reperfusion compared to untreated I/R controls (Figs. 12 and 13, both $P<0.05$). Additionally, I/R hearts treated with 20 μ M MitoQ showed significant improvement in LVDP and dP/dt_{max} by 40 min reperfusion compared to untreated I/R controls (Figs. 12 and 13, both $P<0.05$). However, MitoQ (10, 20 μ M) was not able to significantly restore dP/dt_{min} compared to untreated I/R control hearts (Fig. 14). The I/R hearts treated with a 1 μ M dose of MitoQ did not show any significant changes in LVDP, dP/dt_{max} , or dP/dt_{min} throughout the I/R timecourse (Figs. 12-14).

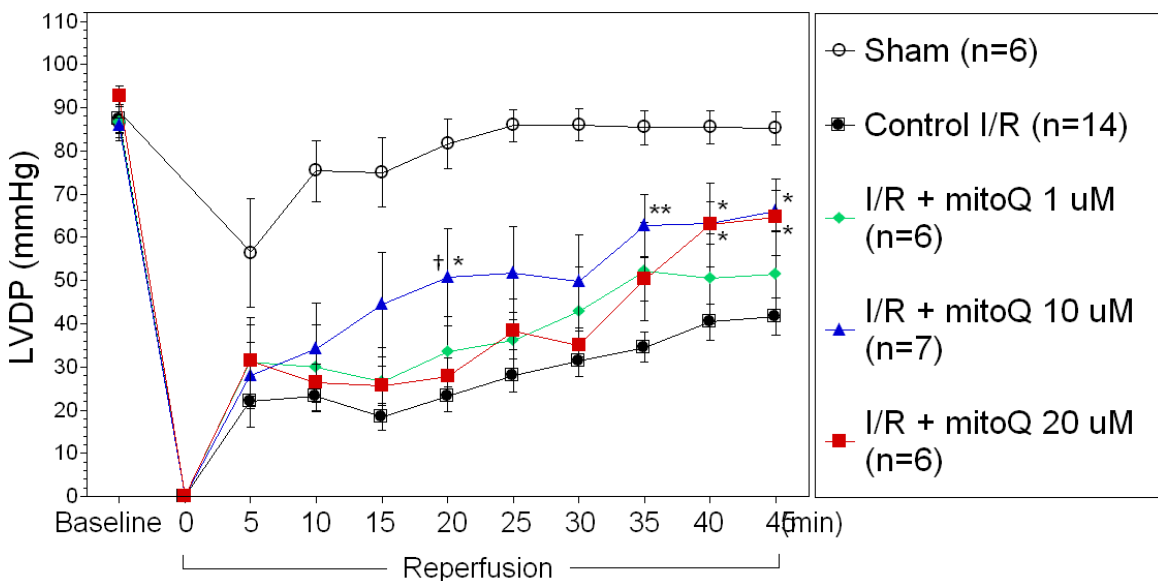


Figure 12. Time course of measurements of left ventricular developed pressure (LVDP) expressed in mmHg from initial baseline period (before ischemia) to the final recording time point (at 45 min reperfusion) from isolated perfused rat hearts ($*P<0.05$, $**P<0.01$ compared to control I/R; $\dagger P<0.05$ compared to MitoQ 20 μ M). All values are expressed as mean \pm SEM.

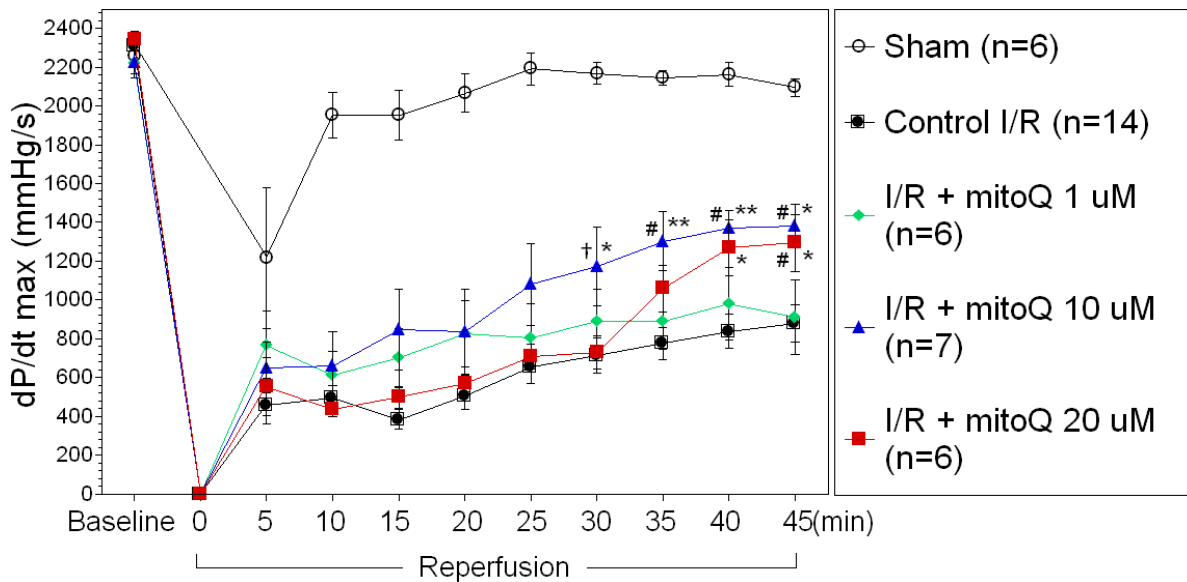


Figure 13. Time course of measurements of the peak rate of rise in the first derivative of left ventricular systolic pressure (dP/dt_{max}) expressed in mmHg/s from initial baseline period (before ischemia) to the final recording time point (at 45 min reperfusion) from isolated perfused rat hearts. (* $P < 0.05$, ** $P < 0.01$ compared to control I/R; # $P < 0.05$; † $P < 0.05$ compared to MitoQ 20 μ M). All values are expressed as mean \pm SEM.

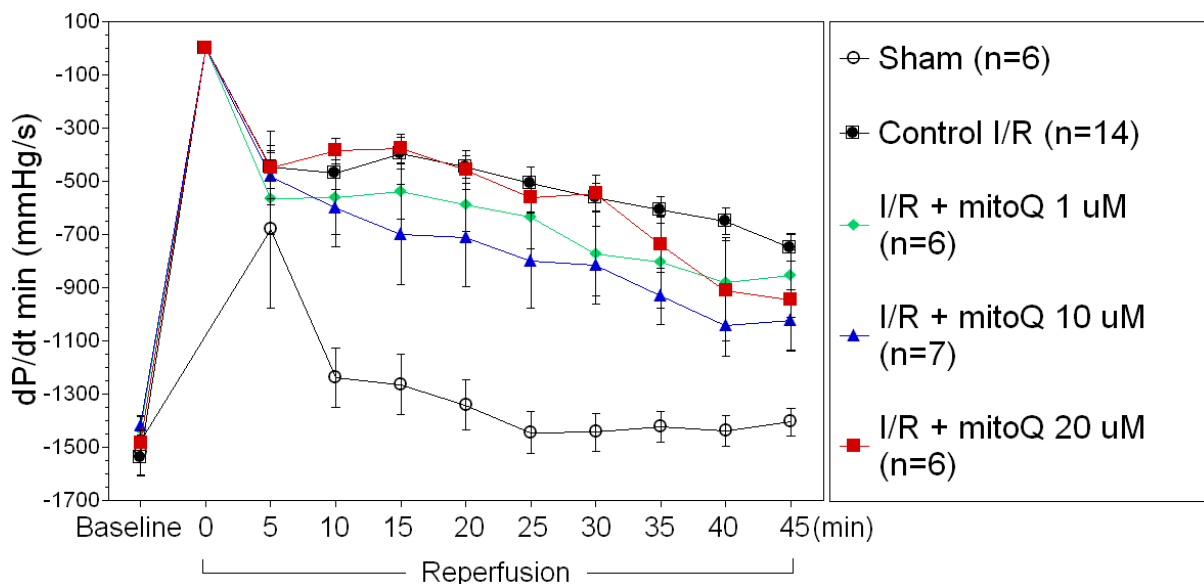


Figure 14. Time course of measurements of the minimal rate of left ventricular systolic pressure in the first derivative (dP/dt_{min}) expressed in mmHg/s from initial baseline period (before ischemia) to the final recording time point (at 45 min reperfusion) from isolated perfused rat hearts. All values are expressed as mean \pm SEM.

I/R + SS-31 (25 μ M, 50 μ M, 100 μ M)

Cardiac Function

Figures 15, 16, and 17 show the initial and final values of LVDP, dP/dt_{max} , and dP/dt_{min} from each experimental group, respectively. There was no statistically significant difference initially between the baseline values between any of the experimental groups. I/R hearts treated with SS-31 50 μ M significantly recovered in LVDP, dP/dt_{max} , and dP/dt_{min} compared to untreated control I/R ($P < 0.01$ compared to untreated control I/R, Table 2, Figs. 15-17); whereas SS-31 (25, 100 μ M) treatment did not show statistical difference from the untreated I/R control (Table 2, Figs. 15-17).

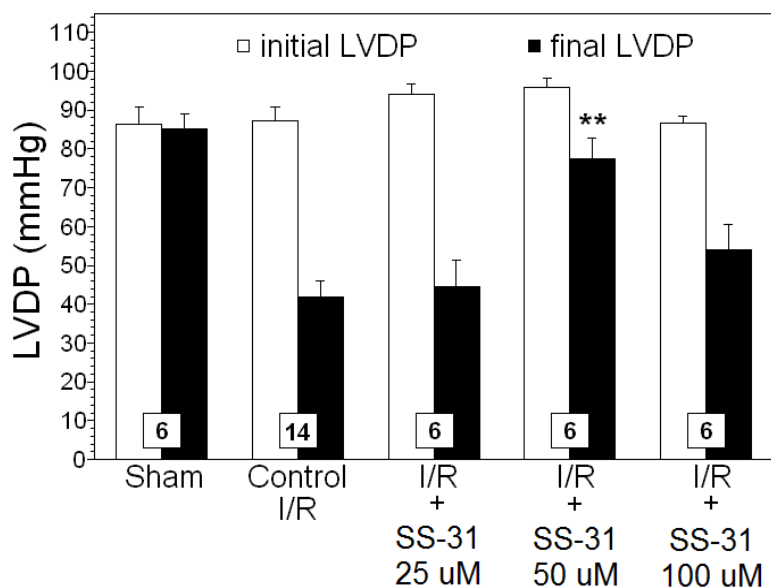


Figure 15. Initial (before ischemia) and final (at 45 min reperfusion) measurements from isolated perfused rat hearts of left ventricular developed pressure (LVDP), expressed in mmHg. (** $P < 0.01$ compared to control I/R). All values are expressed as mean \pm SEM. The number of hearts in each experimental group is shown in the box at the base of each bar.

Figure 16. Initial (before ischemia) and final (at 45 min reperfusion) measurements from isolated perfused rat hearts of the peak rate of rise in the first derivative of left ventricular systolic pressure (dP/dt_{max}), expressed in mmHg/s. (** $P < 0.01$ compared to control I/R). All values are expressed as mean \pm SEM. The number of hearts in each experimental group is shown in the box at the base of each bar.

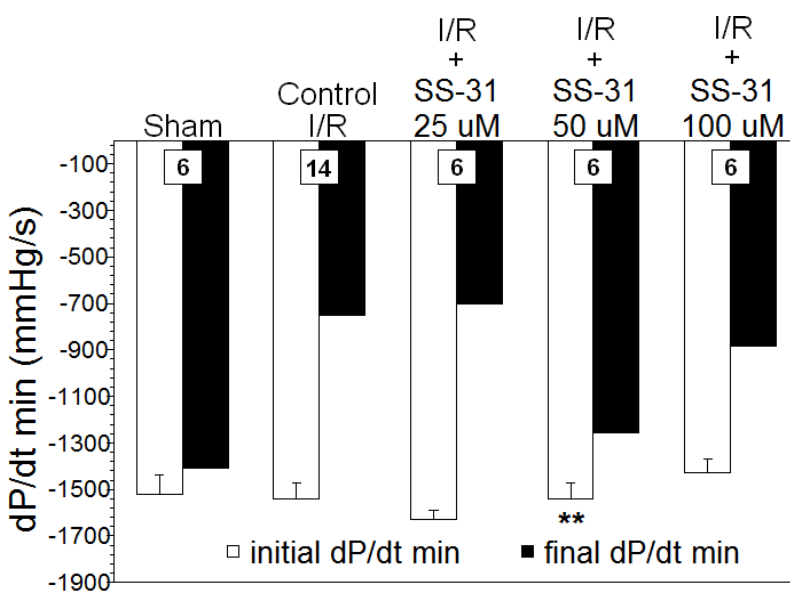
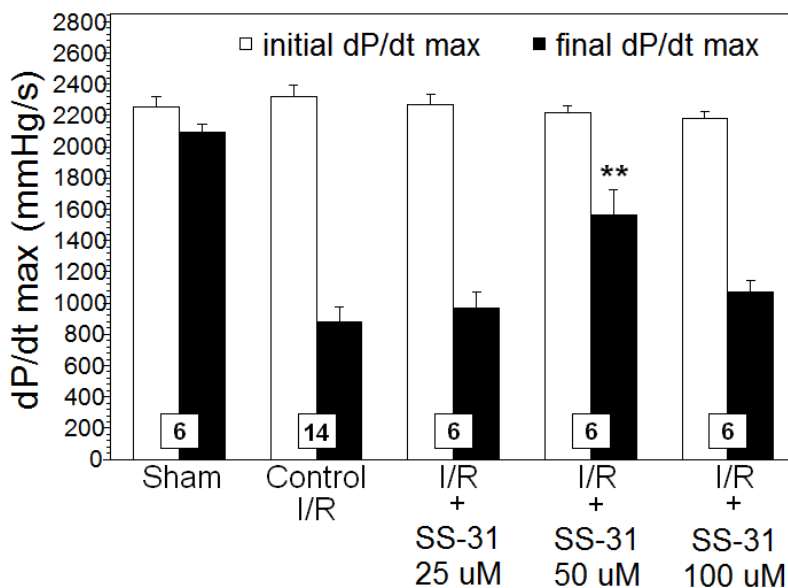


Figure 17. Initial (before ischemia) and final (at 45 min reperfusion) measurements from isolated perfused rat hearts of the minimal rate of left ventricular systolic pressure in the first derivative (dP/dt_{min}) expressed in mmHg/s. (** $P < 0.01$ compared to control I/R). All values are expressed as mean \pm SEM. The number of hearts in each experimental group is shown in the box at the base of each bar.

Moreover, the time courses of LVDP, dP/dt_{max} , and dP/dt_{min} show that the I/R control group exhibited sustained contractile dysfunction throughout the 45 min period of reperfusion following ischemia compared to the sham hearts that did not experience ischemia ($P < 0.01$). However, the I/R hearts treated with 50 μ M SS-31 showed significantly recovered LVDP, dP/dt_{max} , and dP/dt_{min} by the 15

min time point, suggesting that cardiac contractile function can recover more quickly after an infusion of SS-31 (50 μ M) and sustain better contractile function by 45 min of reperfusion compared to untreated I/R controls (Figs. 18-20, all $P < 0.01$).

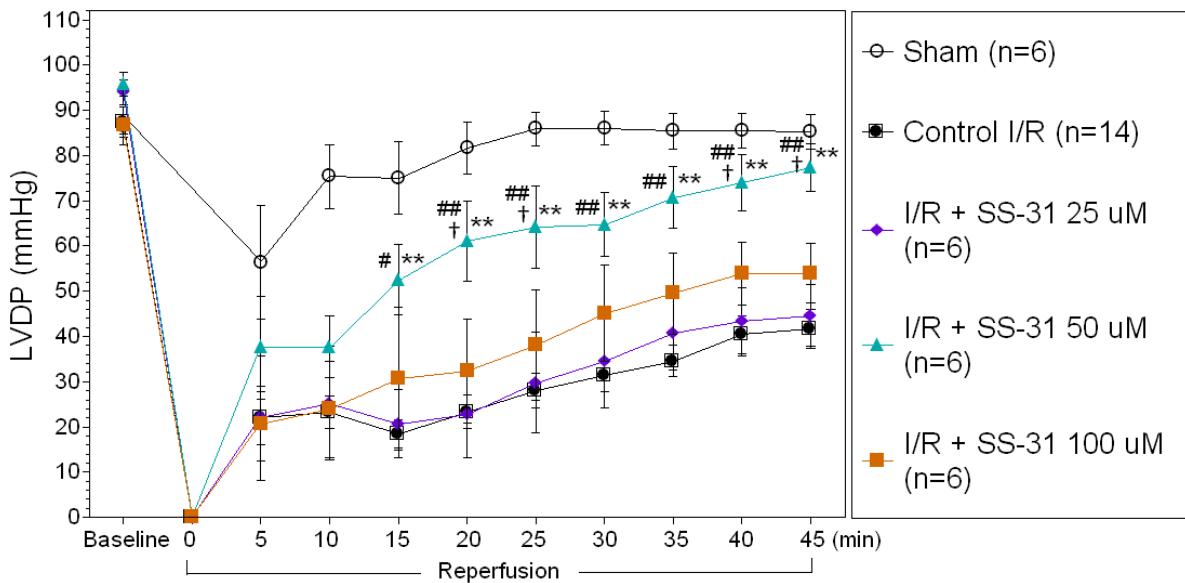


Figure 18. Time course of measurements of left ventricular developed pressure (LVDP) expressed in mmHg from initial baseline period (before ischemia) to the final recording time point (at 45 min reperfusion) from isolated perfused rat hearts. Infusion of SS-31 at reperfusion attenuated cardiac contractile dysfunction by allowing LVDP to recover closer to baseline values throughout the time course of the experiment (** $P < 0.01$ compared to control I/R; # $P < 0.05$, ## $P < 0.01$ compared to SS-31 25 μ M; † $P < 0.05$ compared to SS-31 100 μ M). All values are expressed as mean \pm SEM.

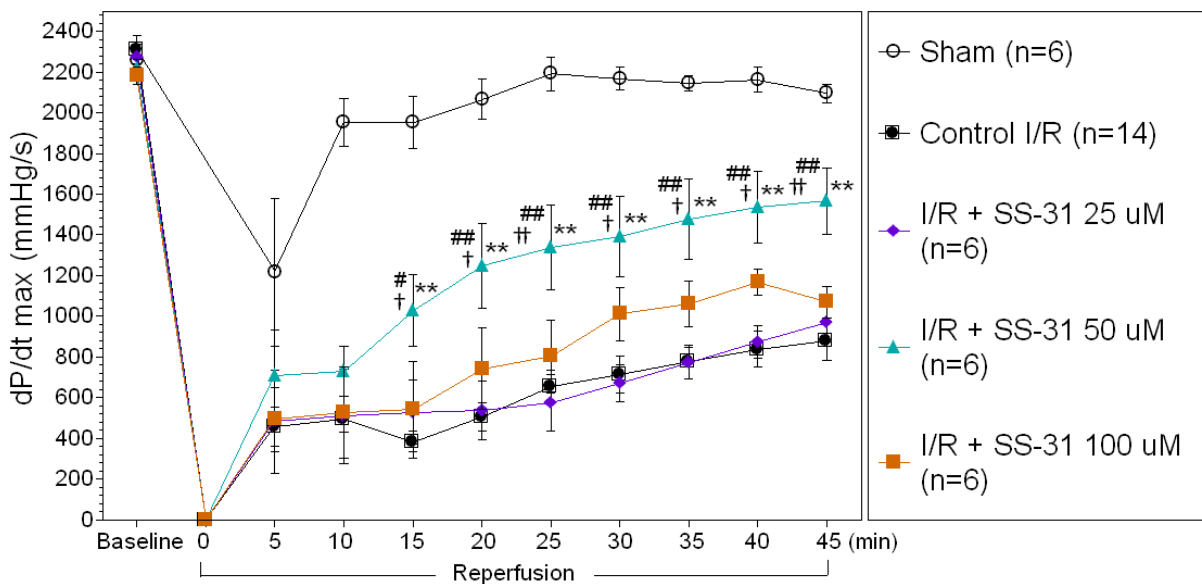


Figure 19. Time course of measurements of the peak rate of rise in the first derivative of left ventricular systolic pressure (dP/dt_{max}) expressed in mmHg/s from initial baseline period (before ischemia) to the final recording time point (at 45 min reperfusion) from isolated perfused rat hearts. Infusion of SS-31 at reperfusion attenuated cardiac contractile dysfunction by allowing dP/dt_{max} to recover closer to baseline values throughout the time course of the experiment (** $P < 0.01$ compared to control I/R; # $P < 0.05$, ## $P < 0.01$ compared to SS-31 25 μM ; † $P < 0.05$, †† $P < 0.01$ compared to SS-31 100 μM). All values are expressed as mean \pm SEM.

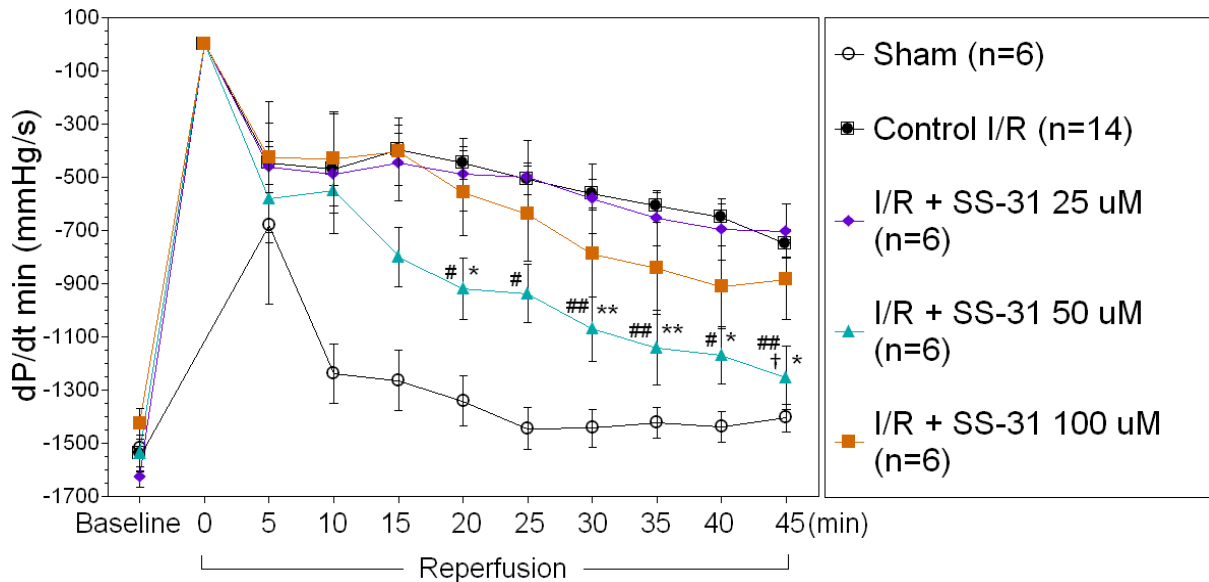


Figure 20. Time course of measurements of the minimal rate of left ventricular systolic pressure in the first derivative (dP/dt_{min}) expressed in mmHg/s from initial baseline period (before ischemia) to the final recording time point (at 45 min reperfusion) from isolated perfused rat hearts. Infusion of SS-31 at reperfusion attenuated cardiac contractile dysfunction by allowing dP/dt_{min} to recover closer to baseline values throughout the time course of the experiment (* $P < 0.05$, ** $P < 0.01$ compared to control I/R; # $P < 0.05$, ## $P < 0.01$ compared to SS-31 25 μM ; † $P < 0.05$ compared to SS-31 100 μM) All values are expressed as mean \pm SEM.

I/R + MitoQ (1 μM , 10 μM , 20 μM) and I/R + SS-31 (25 μM , 50 μM , 100 μM)

Infarct Size

Figure 21 illustrates cross sections of left ventricular tissue stained with 1% TTC to detect infarct size.

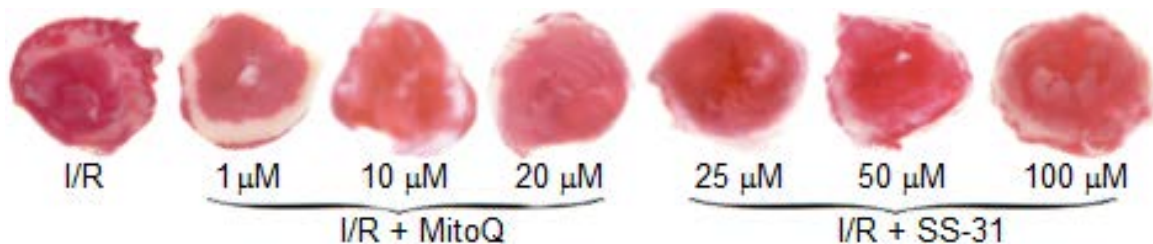


Figure 21. Representative cross sections of I/R left ventricles subjected to TTC staining. Viable tissue stained red while the areas of infarction stained white.

The weight ratio of cardiac tissue infarct to the total area at risk was calculated and statistically analyzed. The I/R hearts treated with MitoQ (10 μ M and 20 μ M) or SS-31 (25, 50, 100 μ M) showed a significantly smaller infarct size compared to untreated I/R controls ($P < 0.01$ compared to control I/R; Table 2, Fig. 22). These results suggest that the infusion of MitoQ or SS-31 at reperfusion significantly reduces the amount of cardiac tissue death following I/R. However, the I/R hearts treated with 1 μ M MitoQ did not show a significant difference in infarct size compared to untreated I/R hearts, suggesting that there is no cardioprotective effect at this dose (Fig. 22).

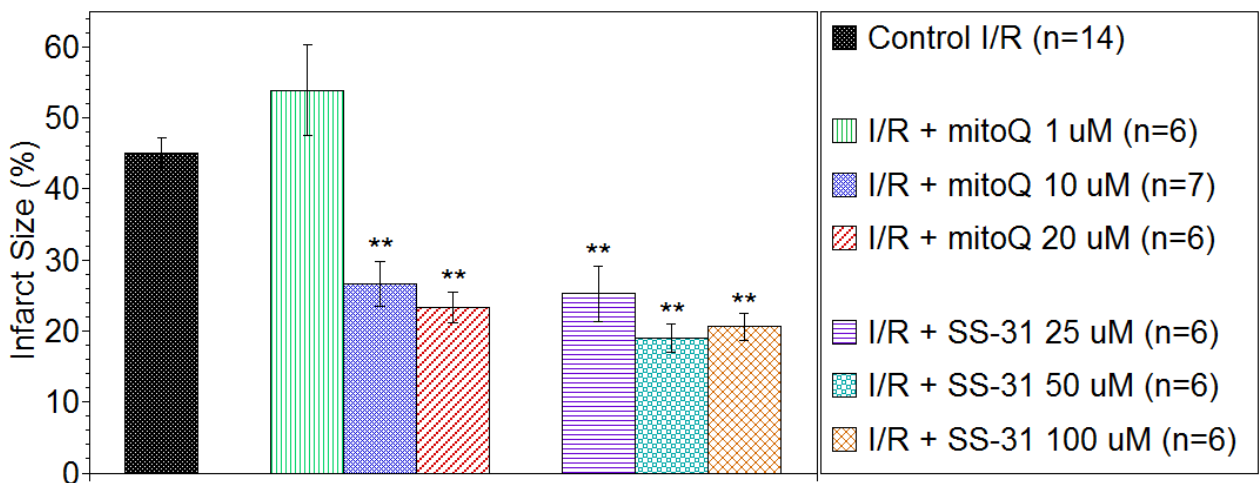


Figure 22. Ratio of infarct size to total cardiac tissue at risk as determined by TTC staining. Infusion of MitoQ (10, 20 μ M) or SS-31 (25, 50, 100 μ M) at reperfusion attenuated cardiac tissue death compared to untreated I/R hearts (* $P < 0.05$, ** $P < 0.01$). All values are expressed as mean \pm SEM.

DISCUSSION

Summary of major findings

The results of this study suggest the infusion of MitoQ (10, 20 μ M) at reperfusion improves postreperfused cardiac contractile function compared to I/R control hearts. The effect of MitoQ on cardiac function correlates with the infarct size data, suggesting the effects of the infusion of MitoQ at reperfusion can range from 1 to 20 μ M. By contrast, all SS-31 treated I/R hearts showed a reduction in infarct size compared to the untreated control I/R hearts, but only the 50 μ M dose of SS-31 elicited improvement in cardiac function within the 45 minute reperfusion period. This result is consistent with a previous myocardial I/R study in which a SS-31 analog (i.e., Bendavia) showed a reduction in infarct size but no significant improvement in cardiac function(95). Kloner et al. suggest SS peptides can reduce infarct size in I/R but may not improve post-reperfused cardiac function because the myocardium may be reversibly stunned and require more time to improve. Similarly, in this myocardial I/R study, SS-31 significantly reduced infarct size compared to the untreated control I/R hearts, yet the 25 and 100 μ M doses of SS-31 could not restore cardiac function within the 45 minute reperfusion period as quickly as the 50 μ M dose of SS-31. Since it has been suggested that most I/R-induced damage occurs within the first 5 minutes of reperfusion, it is important to discover agents that can work rapidly and effectively to reduce the amount of I/R injury(8, 9).

These results suggest that mitochondrial ROS may be a significant contributor to myocardial I/R injury and are consistent with the hypothesis that inhibiting the release and accumulation of excess mitochondrial ROS with MitoQ or SS-31 attenuates myocardial I/R injury and subsequent cardiac contractile dysfunction and tissue death.

The effects of MitoQ on cardiac contractile function and infarct size in I/R

The administration of MitoQ (10, 20 μ M) at reperfusion significantly restored postreperfused LVDP and dP/dt_{max} closer to baseline levels and reduced infarct size in comparison to untreated I/R hearts. Although the 10 and 20 μ M doses of MitoQ significantly restored LVDP and dP/dt_{max} ($P < 0.05$), none of the doses of MitoQ significantly restored postreperfused dP/dt_{min} in comparison to I/R controls. This finding suggests that postreperfused MitoQ treated hearts reach maximum contractility quickly but relax at a rate comparable to that of postreperfused untreated I/R hearts. MitoQ (10, 20 μ M) administered at reperfusion was able to allow LVDP to recover more closely to baseline values after 45 min reperfusion than untreated I/R hearts. Although there was no significant difference in LVEDP between the experimental groups at the final time point in these experiments, lower post-I/R LVEDP could possibly contribute to the improved LVDP recovery in MitoQ-treated hearts. Although the I/R hearts treated with 20 μ M of MitoQ reached final contractile function measurements similar to those of the I/R hearts treated with 10 μ M, the time course of the I/R hearts treated with 20 μ M showed that these hearts did not significantly differ from

untreated control I/R hearts in the 5-35 min period of reperfusion. In contrast, the I/R hearts treated with 10 μM of MitoQ significantly improved in LVDP by the 15 min time point and in dP/dt_{max} by the 30 min time point. This delay in effect of the 20 μM dose of MitoQ could possibly be attributed to reversible dysfunction in viable cells since these hearts significantly recovered LVDP and dP/dt_{max} by 45 min reperfusion and also had a significantly smaller infarct size compared to untreated control I/R hearts. There was no statistical significance between MitoQ (1, 10, 20 μM) and untreated I/R hearts in the heart rate, coronary flow, LVESP, or LVEDP final values. While it would be expected that a decrease in infarct size would correlate with an increase in coronary flow, such an effect was not evident in this study(89, 95-97). In summary, postreperfused MitoQ-treated I/R hearts display significantly restored cardiac contractile function and smaller infarct size than untreated I/R hearts. These results suggest that mitochondrial ROS may be a significant contributor to myocardial I/R injury, and inhibiting the release of mitochondrial ROS with selective mitochondria-targeted antioxidants attenuates myocardial I/R injury and subsequent cardiac contractile dysfunction.

These results are consistent with the findings of other studies in which MitoQ attenuated tissue damage and dysfunction in I/R models. The Adlam et al. 2005 study reported that a pretreatment of MitoQ (500 μM) in drinking water given to rats for two weeks prior to I(30min)/R(60min) improved postreperfused cardiac function in isolated rat hearts compared to I/R control hearts. Specifically, MitoQ-treated rat hearts achieved a significantly improved recovery of postreperfused LVDP in comparison to treatment with untargeted antioxidant compounds(16). A

similar study using pretreatment with MitoQ (500 μ M) in drinking water for 10 days prior to I(20min)/R(90min) in isolated perfused rat hearts showed an improvement in LVDP by 20% compared to I/R control hearts(74). The response to myocardial I/R of the MitoQ pretreated isolated perfused hearts in these studies suggests that mitochondria-derived ROS is a source of oxidative stress implicated in myocardial I/R injury.

The cardioprotective effects attributed to MitoQ were also investigated in another study in which rats were treated with doxorubicin (DOX), a drug known to induce cardiomyopathy, and MitoQ. These rats were treated for 12 weeks with DOX, MitoQ, or DOX plus MitoQ. Two-dimensional echocardiography measured the left ventricular function, which decreased in DOX-treated rats but was preserved during MitoQ plus DOX treatment. In addition, cytochrome c oxidase function was restored in DOX plus MitoQ (2 mg/kg) rats but diminished in DOX-treated rats(98). The dose of MitoQ administered in the DOX-treated rat study is similar to the dose range used by our research group to show a reduction in rat blood H₂O₂ levels when administered during reperfusion compared to untreated I/R controls(99). In a hypertensive rat model of cardiovascular disease, MitoQ reduced cardiac dysfunction, blood pressure, cardiac hypertrophy, and endothelial dysfunction(100). Bovine aortic endothelial cells pretreated with MitoQ (1 μ M) and incubated with glucose/glucose oxidase, to induce caspase activation, inhibited H₂O₂-induced apoptosis and lipid and protein peroxidation while also preserving mitochondrial membrane potential(101). Although pretreatment with MitoQ in these studies exhibited significant cardioprotective

effects, administering MitoQ as a pretreatment may not be a practical option in clinical occurrences of myocardial infarction. Therefore, administering MitoQ at reperfusion may prove more useful. MitoQ has exhibited protective effects when given during reperfusion following one hour ischemia in liver I/R and resulted in reduced ALT and AST liver enzymes immediately following ischemia and throughout a 24 hour reperfusion. Consequently, a smaller percentage of damaged liver tissue was found in the MitoQ treatment group(30). The concentration of MitoQ used in this liver I/R model was similar to the doses of MitoQ used in our *in vivo* hind limb I/R and *ex vivo* myocardial I/R models, which showed that MitoQ can reduce blood H₂O₂ levels and infarct size, respectively, in I/R(99, 102). Antioxidants that are targeted specifically to mitochondria, especially those that work rapidly and achieve efficacy when administered upon reperfusion, may be useful clinically in reducing mitochondrial oxidative damage following the reperfusion of ischemic tissue.

The effects of SS-31 on cardiac contractile function and infarct size in I/R

SS-31 (50 μ M, P<0.01) administered at reperfusion also significantly restored postreperfused cardiac contractile function parameters, LVDP, dP/dt_{max}, and dP/dt_{min}, significantly compared to untreated I/R hearts. There was no statistical significance between SS-31 (25, 50, 100 μ M) and untreated I/R hearts in the heart rate, coronary flow, LVESP, or LVEDP final values. Administration of SS-31 (25, 50, 100 μ M; P<0.01) at reperfusion significantly reduced infarct size compared to untreated I/R hearts. Unexpectedly, the administration of the 25 and

100 μM doses of SS-31 at reperfusion did not have significant restoration in cardiac function compared to untreated I/R hearts, but there was a significant decrease in infarct size in these I/R hearts ($P < 0.01$). This anomaly could potentially be attributed to reversible I/R-induced myocardial stunning. Reversibly stunned myocardium is mechanically arrhythmic but could possibly regain function at a later time. Dysfunction in viable cells could potentially be reversed, whereas infarction is irreversible. Therefore, it is possible that cardiac function could improve or decline at a time point beyond the time course recorded in this study. This anomaly is consistent with the findings of a study investigating the cardioprotective effects of Bendavia, an analogue of SS-31 and SS-02, in myocardial I/R. The study found that treatment with Bendavia reduced infarct size in guinea pig and sheep myocardial I/R models. However, there was no effect on left ventricular output or arrhythmia score compared to untreated I/R animals. It has been suggested that the surviving myocardium surrounding an infarct may remain stunned for days to weeks following I/R(95). This explanation may account for why the 25 and 100 μM doses of SS-31 did not significantly improve post-reperfused cardiac function despite significantly decreasing infarct size compared to untreated I/R controls(102). The results of the present study suggest that mitochondrial ROS may be a significant contributor to myocardial I/R injury, and inhibiting the release of mitochondrial ROS with selective mitochondria-targeted antioxidants attenuates myocardial I/R injury and may have a beneficial effect on subsequent cardiac contractile dysfunction.

The efficacy of SS-31 has been attributed to its ability to become selectively concentrated within mitochondria to scavenge ROS, whereas SS-20 is targeted to mitochondria but unable to scavenge ROS because lacks a Dmt amino acid residue(18, 26, 103). Administration as a pretreatment followed by a second treatment at reperfusion with SS-31 (i.p.), similar in dosage to the SS-31 that reduced blood H₂O₂ in an *in vivo* hind limb I/R model, was able to significantly reduce infarct size, ventricular arrhythmias, and lipid peroxidation in a rat myocardial I(60min)/R(60min) model *in vivo*(75, 99). A study using an *ex vivo* guinea pig global myocardial I(30min)/R(90) model showed SS-31 is able to prevent myocardial stunning when given throughout the experiment effectively, and these results were later obtained with an SS-31 analog using an *in vivo* myocardial I/R model(8, 73, 82, 104). The results from this study are unique in that SS-31 was administered exclusively at reperfusion and still able to improve infarct size and post-reperfused cardiac function; administration at the time of reperfusion may be more clinically relevant in cases of patients experiencing myocardial infarction(102). These results suggest that mitochondrial-derived ROS is a significant contributing factor to myocardial stunning, and reduction in mitochondrial ROS is cardioprotective. Similarly, SS-31 (2 mg/kg, i.p.) administered at reperfusion in a mouse cerebral I(30min)/R(72h) model significantly reduced infarct size compared to the untreated I/R brains(87, 105). The activity of tert-butyl hydroperoxide, known to induce mitochondrial depolarization and apoptosis by lipid peroxidation, was reduced in neuronal cell lines also treated with SS-31. SS-31 also exhibited ROS-scavenging activity in

the same neuronal cell lines(26). A subcutaneous pretreatment, treatment at reperfusion, and post treatment with SS-31 in a rat kidney I(30-45min)/R(24h) model resulted in preserved mitochondrial structure and function as well as reduced oxidative stress and inflammation following I/R(18). In hepatocytes treated with hypochlorous acid, SS-31 was able to prevent cell death by inhibiting an increase in mitochondrial SO and mitochondrial depolarization(106). SS-31 was also able to prevent an increase in mitochondrial SO due to induced shear stress in endothelial cells(107). SS-31 has also been effective in a chronic model of cardiac dysfunction by alleviating hypertensive cardiomyopathy. In the study, SS-31 was able to significantly reduce angiotensin II-induced mitochondrial oxidative stress, apoptosis signaling, and fibrosis(22). Furthermore, SS-31 is also able to promote the activity of mitochondrial respiration and synthesis of ATP in addition to its ability to scavenge ROS and attenuate ROS production and mitochondrial swelling(108, 109).

Future Studies

To more clearly understand the role of mitochondrial-derived ROS in contributing to myocardial I/R injury, direct measurements of mitochondrial ROS at various I/R time points may allow clarification of the correlation between the amount of ROS release and tissue damage in myocardial I/R. These types of measurements may also quantify the efficacy of selectively mitochondrial-targeted antioxidants in reducing mitochondrial ROS release. In a similar way, infarct size could be measured at more than one time point to confirm the ratio of

tissue death that occurs during the reperfusion phase to the ischemic phase of I/R. To supplement the infarct size data, histological staining for apoptosis markers may be useful to confirm areas of cell death. No sham hearts in this study were given SS-31 treatment, which may be a useful way to confirm whether or not SS-31 itself alters cardiac function independently from I/R. Other selectively mitochondrial-targeted antioxidants may also be used in a similar myocardial I/R model. Additionally, eNOS uncoupling has been shown to contribute to I/R injury by initiating endothelial dysfunction and increased ROS release within 5-10 min of reperfusion(52, 53). Measurements of the eNOS dimer to monomer ratio via western blotting of left ventricular tissue or high performance liquid chromatography to detect the BH₄ to BH₂ ratio may be useful in monitoring the degree of eNOS activity in myocardial I/R and understanding the relationship between endothelial dysfunction and myocardial I/R injury.

For more effective translation into the clinical setting, the cardioprotective effects of agents given at reperfusion need to be reproducible in multiple laboratories, models, and species. One of the limitations of the isolated perfused heart model is that there is a limited time course. Measurements of infarct size and cardiac function at time points 24 hours or longer may be better predictors of morbidity and mortality following acute myocardial infarction. I/R-induced myocardial stunning may mask the potential function of postreperfused cardiac tissue since stunning can be reversible. An in vivo regional I/R model could also be used to confirm the results of a global ischemia model and obtain measurements at later time points. Most studies of myocardial I/R use healthy,

juvenile animals without comorbid conditions or varying nutritional or hormonal status(5). Comorbid conditions, such as diabetes, hypertension, hypercholesterolemia, and left ventricular hypertrophy, are commonly found in the clinical setting and may impact the efficacy of cardioprotective interventions(5, 110, 111). Patients in the clinical setting may also have been exposed to transient periods of angina with a preconditioning effect, which can skew the interpretation of how much of the cardioprotective effect can be contributed to an intervention(5).

Significance of Findings

Selectively mitochondrial-targeted antioxidants administered at the time of reperfusion in myocardial I/R exerted cardioprotective effects in this study. MitoQ and SS-31 infused with autologous plasma at the beginning of reperfusion both, independently, expeditiously and effectively restored postreperfused cardiac contractile function and reduced infarct size. The results of this study suggest that MitoQ and SS-31 may effectively reduce I/R injury during the treatment of myocardial infarction or heart transplantation in the clinical setting, thus allowing these patients to have a better quality of life attributable to better cardiac function and more viable cardiac tissue following ischemic events.

FOOTNOTES

This study was supported by the Department of Biomedical Sciences and the Center for Chronic Disorders of Aging (CCDA) at the Philadelphia College of Osteopathic Medicine.

REFERENCES

1. Bayeva M, Gheorghiade M, Ardehali H. Mitochondria as a therapeutic target in heart failure. *J Am Coll Cardiol*. 2013 2/12;61(6):599-610.
2. The top 10 causes of death [Internet].; 2011 []. Available from: <http://www.who.int/mediacentre/factsheets/fs310/en/index.html>.
3. Hoyert DL, Xu J. Deaths: Preliminary data for 2011. National Vital Statistics Report. Hyattsville, MD: National Center for Health Statistics; 2012. Report No.: 61(6).
4. Hausenloy DJ, Yellon DM. Myocardial ischemia-reperfusion injury: A neglected therapeutic target. *J Clin Invest*. 2013 Jan 2;123(1):92-100.
5. Bolli R, Becker L, Gross G, Mentzer R, Jr, Balshaw D, Lathrop DA, et al. Myocardial protection at a crossroads: The need for translation into clinical therapy. *Circ Res*. 2004 Jul 23;95(2):125-34.
6. Ide T, Tsutsui H, Hayashidani S, Kang D, Suematsu N, Nakamura K-, et al. Mitochondrial DNA damage and dysfunction associated with oxidative stress in failing hearts after myocardial infarction. *Circ Res*. 2001;88(5):529-35.
7. Spinale FG, Schulte BA, Crawford FA. Demonstration of early ischemic injury in porcine right ventricular myocardium. *Am J Pathol*. 1989 Mar;134(3):693-704.
8. Wu D, Soong Y, Zhao GM, Szeto HH. A highly potent peptide analgesic that protects against ischemia-reperfusion-induced myocardial stunning. *Am J Physiol Heart Circ Physiol*. 2002 Aug;283(2):H783-91.
9. Becker LB. New concepts in reactive oxygen species and cardiovascular reperfusion physiology. *Cardiovasc Res*. 2004 Feb 15;61(3):461-70.
10. Yellon DM, Hausenloy DJ. Myocardial reperfusion injury. *N Engl J Med*. 2007;357(11):1121,1135+1074.
11. Piper HM, Garcia-Dorado D, Ovize M. A fresh look at reperfusion injury. *Cardiovasc Res*. 1998 May;38(2):291-300.
12. Szeto HH, Schiller PW. Novel therapies targeting inner mitochondrial membrane- from discovery to clinical development. *Pharm Res*. 2011;28(11):2669-79.
13. Jennings RB, Sommers HM, Smyth GA, Flack HA, Linn H. Myocardial necrosis induced by temporary occlusion of a coronary artery in the dog. *Arch Pathol*. 1960 Jul;70:68-78.

14. Szeto HH. Mitochondria-targeted peptide antioxidants: Novel neuroprotective agents. *AAPS Journal*. 2006;8(3):521-31.
15. Szeto HH. Cell-permeable, mitochondrial-targeted, peptide antioxidants. *AAPS Journal*. 2006;8(2):E277-83.
16. Adlam VJ, Harrison JC, Porteous CM, James AM, Smith RAJ, Murphy MP, et al. Targeting an antioxidant to mitochondria decreases cardiac ischemia-reperfusion injury. *FASEB Journal*. 2005;19(9):1088-95.
17. Rodriguez-Cuenca S, Cochemé HM, Logan A, Abakumova I, Prime TA, Rose C, et al. Consequences of long-term oral administration of the mitochondria-targeted antioxidant MitoQ to wild-type mice. *Free Radical Biology and Medicine*. 2010;48(1):161-72.
18. Szeto HH, Liu S, Soong Y, Wu D, Darrah SF, Cheng F-, et al. Mitochondria-targeted peptide accelerates ATP recovery and reduces ischemic kidney injury. *J Am Soc Nephrol*. 2011;22(6):1041-52.
19. Szeto HH. Mitochondria-targeted cytoprotective peptides for ischemia-reperfusion injury. *Antioxidants and Redox Signaling*. 2008;10(3):601-19.
20. Cho J, Won K, Wu D, Soong Y, Liu S, Szeto HH, et al. Potent mitochondria-targeted peptides reduce myocardial infarction in rats. *Coron Artery Dis*. 2007;18(3):215-20.
21. Ide T, Tsutsui H, Kinugawa S, Utsumi H, Kang D, Hattori N, et al. Mitochondrial electron transport complex I is a potential source of oxygen free radicals in the failing myocardium. *Circ Res*. 1999;85(4):357-63.
22. Dai D-, Chen T, Szeto H, Nieves-Cintrón M, Kutuyavin V, Santana LF, et al. Mitochondrial targeted antioxidant peptide ameliorates hypertensive cardiomyopathy. *J Am Coll Cardiol*. 2011;58(1):73-82.
23. Ide T, Tsutsui H, Hayashidani S, Kang D, Suematsu N, Nakamura K-, et al. Mitochondrial DNA damage and dysfunction associated with oxidative stress in failing hearts after myocardial infarction. *Circ Res*. 2001;88(5):529-35.
24. Siwik DA, Colucci WS. Regulation of matrix metalloproteinases by cytokines and reactive oxygen/nitrogen species in the myocardium. *Heart Fail Rev*. 2004;9(1):43-51.
25. Czerski LW, Szweda PA, Szweda LI. Dissociation of cytochrome c from the inner mitochondrial membrane during cardiac ischemia. *J Biol Chem*. 2003;278(36):34499-504.
26. Zhao K, Luo G, Giannelli S, Szeto HH. Mitochondria-targeted peptide prevents mitochondrial depolarization and apoptosis induced by tert-butyl hydroperoxide in neuronal cell lines. *Biochem Pharmacol*. 2005 Dec 5;70(12):1796-806.

27. Lemasters JJ, Bond JM, Chacon E, Harper IS, Kaplan SH, Ohata H, et al. The pH paradox in ischemia-reperfusion injury to cardiac myocytes. *EXS*. 1996;76:99-114.
28. Ide T, Tsutsui H, Kinugawa S, Utsumi H, Kang D, Hattori N, et al. Mitochondrial electron transport complex I is a potential source of oxygen free radicals in the failing myocardium. *Circ Res*. 1999;85(4):357-63.
29. Schmidt TS, Alp NJ. Mechanisms for the role of tetrahydrobiopterin in endothelial function and vascular disease. *Clin Sci*. 2007;113(1-2):47-63.
30. Mukhopadhyay P, Horváth B, Zsengeller Z, Bátkai S, Cao Z, Kechrid M, et al. Mitochondrial reactive oxygen species generation triggers inflammatory response and tissue injury associated with hepatic ischemiareperfusion: Therapeutic potential of mitochondrially targeted antioxidants. *Free Radical Biology and Medicine*. 2012;53(5):1123-38.
31. Kwon SH, Pimentel DR, Remondino A, Sawyer DB, Colucci WS. H₂O₂ regulates cardiac myocyte phenotype via concentration-dependent activation of distinct kinase pathways. *J Mol Cell Cardiol*. 2003;35(6):615-21.
32. Sawyer DB, Siwik DA, Xiao L, Pimentel DR, Singh K, Colucci WS. Role of oxidative stress in myocardial hypertrophy and failure. *J Mol Cell Cardiol*. 2002 Apr;34(4):379-88.
33. Finkel T. Redox-dependent signal transduction. *FEBS Lett*. 2000 Jun 30;476(1-2):52-4.
34. Chiu HY, Tsao LY, Yang RC. Heat-shock response protects peripheral blood mononuclear cells (PBMCs) from hydrogen peroxide-induced mitochondrial disturbance. *Cell Stress Chaperones*. 2009 Mar;14(2):207-17.
35. Wei S, Rothstein EC, Fliegel L, Dell'Italia LJ, Lucchesi PA. Differential MAP kinase activation and Na⁺/H⁺ exchanger phosphorylation by H₂O₂ in rat cardiac myocytes. *Am J Physiol Cell Physiol*. 2001 Nov;281(5):C1542-50.
36. Sugden PH, Clerk A. "Stress-responsive" mitogen-activated protein kinases (c-jun N-terminal kinases and p38 mitogen-activated protein kinases) in the myocardium. *Circ Res*. 1998 Aug 24;83(4):345-52.
37. Siwik DA, Tzortzis JD, Pimental DR, Chang DL, Pagano PJ, Singh K, et al. Inhibition of copper-zinc superoxide dismutase induces cell growth, hypertrophic phenotype, and apoptosis in neonatal rat cardiac myocytes in vitro. *Circ Res*. 1999 Jul 23;85(2):147-53.
38. Pimentel DR, Amin JK, Xiao L, Miller T, Viereck J, Oliver-Krasinski J, et al. Reactive oxygen species mediate amplitude-dependent hypertrophic and apoptotic responses to mechanical stretch in cardiac myocytes. *Circ Res*. 2001 Aug 31;89(5):453-60.
39. von Harsdorf R, Li PF, Dietz R. Signaling pathways in reactive oxygen species-induced cardiomyocyte apoptosis. *Circulation*. 1999 Jun 8;99(22):2934-41.

40. Chen QM, Tu VC, Wu Y, Bahl JJ. Hydrogen peroxide dose dependent induction of cell death or hypertrophy in cardiomyocytes. *Arch Biochem Biophys*. 2000 Jan 1;373(1):242-8.
41. Vieira HLA, Belzacq A-, Haouzi D, Bernassola F, Cohen I, Jacotot E, et al. The adenine nucleotide translocator: A target of nitric oxide, peroxynitrite, and 4-hydroxynonenal. *Oncogene*. 2001;20(32):4305-16.
42. Vieira HLA, Belzacq A-, Haouzi D, Bernassola F, Cohen I, Jacotot E, et al. The adenine nucleotide translocator: A target of nitric oxide, peroxynitrite, and 4-hydroxynonenal. *Oncogene*. 2001;20(32):4305-16.
43. Shen W, Tian R, Saupe KW, Spindler M, Ingwall JS. Endogenous nitric oxide enhances coupling between O₂ consumption and ATP synthesis in guinea pig hearts. *Am J Physiol Heart Circ Physiol*. 2001 Aug;281(2):H838-46.
44. Lambeth JD. NOX enzymes and the biology of reactive oxygen. *Nature Reviews Immunology*. 2004;4(3):181-9.
45. Ago T, Kuroda J, Pain J, Fu C, Li H, Sadoshima J. Upregulation of Nox4 by hypertrophic stimuli promotes apoptosis and mitochondrial dysfunction in cardiac myocytes. *Circ Res*. 2010;106(7):1253-64.
46. Kuroda J, Ago T, Matsushima S, Zhai P, Schneider MD, Sadoshima J. NADPH oxidase 4 (Nox4) is a major source of oxidative stress in the failing heart. *Proc Natl Acad Sci U S A*. 2010;107(35):15565-70.
47. Heymes C, Bendall JK, Ratajczak P, Cave AC, Samuel J-, Hasenfuss G, et al. Increased myocardial NADPH oxidase activity in human heart failure. *J Am Coll Cardiol*. 2003;41(12):2164-71.
48. Doerries C, Grote K, Hilfiker-Kleiner D, Luchtefeld M, Schaefer A, Holland SM, et al. Critical role of the NAD(P)H oxidase subunit p47phox for left ventricular remodeling/dysfunction and survival after myocardial infarction. *Circ Res*. 2007;100(6):894-903.
49. Ago T, Kuroda J, Pain J, Fu C, Li H, Sadoshima J. Upregulation of Nox4 by hypertrophic stimuli promotes apoptosis and mitochondrial dysfunction in cardiac myocytes. *Circ Res*. 2010;106(7):1253-64.
50. Montgomery M, Adams J, Teng J, Tekelehaymanot B, Ondrasik R, Devine I, et al. Myristoylated protein kinase C epsilon peptide inhibitor exerts cardioprotective effects in rat and porcine myocardial ischemia/reperfusion: A translational research study. *Peptides Across the Pacific: The Proceedings of the Twenty-Third American and Sixth International Peptide Symposium*. 2013:178-9.
51. Schuh A, Liehn EA, Sasse A, Schneider R, Neuss S, Weber C, et al. Improved left ventricular function after transplantation of microspheres and fibroblasts in a rat model of myocardial infarction. *Basic Res Cardiol*. 2009;104(4):403-11.

52. Perkins K-A, Pershad S, Chen Q, McGraw S, Adams JS, Zambrano C, et al. The effects of modulating eNOS activity and coupling in ischemia/reperfusion (I/R). *Naunyn Schmiedeberg's Arch Pharmacol*. 2012;385(1):27-38.
53. Lefer AM, Lefer DJ. The role of nitric oxide and cell adhesion molecules on the microcirculation in ischaemia-reperfusion. *Cardiovasc Res*. 1996;32(4):743-51.
54. Moens AL, Takimoto E, Tocchetti CG, Chakir K, Bedja D, Cormaci G, et al. Reversal of cardiac hypertrophy and fibrosis from pressure overload by tetrahydrobiopterin efficacy of recoupling nitric oxide synthase as a therapeutic strategy. *Circulation*. 2008;117(20):2626-36.
55. Moens AL, Champion HC, Claeys MJ, Tavazzi B, Kaminski PM, Wolin MS, et al. High-dose folic acid pretreatment blunts cardiac dysfunction during ischemia coupled to maintenance of high-energy phosphates and reduces postreperfusion injury. *Circulation*. 2008;117(14):1810-9.
56. Clementi E, Nisoli E. Nitric oxide and mitochondrial biogenesis: A key to long-term regulation of cellular metabolism. *Comparative Biochemistry and Physiology - A Molecular and Integrative Physiology*. 2005;142(2):102-10.
57. Brown GC. Nitric oxide and mitochondria. *Frontiers in Bioscience*. 2007;12(3):1024-33.
58. Garnier A, Fortin D, Deloménie C, Momken I, Veksler V, Ventura-Clapier R. Depressed mitochondrial transcription factors and oxidative capacity in rat failing cardiac and skeletal muscles. *J Physiol (Lond)*. 2003;551(2):491-501.
59. Witt H, Schubert C, Jaekel J, Fliegner D, Penkalla A, Tiemann K, et al. Sex-specific pathways in early cardiac response to pressure overload in mice. *Journal of Molecular Medicine*. 2008;86(9):1013-24.
60. Faerber G, Barreto-Perreia F, Schoepe M, Gilsbach R, Schreppe A, Schwarzer M, et al. Induction of heart failure by minimally invasive aortic constriction in mice: Reduced peroxisome proliferator-activated receptor γ coactivator levels and mitochondrial dysfunction. *J Thorac Cardiovasc Surg*. 2011;141(2):492-500.
61. Marín-García J, Goldenthal MJ, Damle S, Pi Y, Moe GW. Regional distribution of mitochondrial dysfunction and apoptotic remodeling in pacing-induced heart failure. *J Card Fail*. 2009;15(8):700-8.
62. Sebastiani M, Giordano C, Nediani C, Travaglini C, Borchi E, Zani M, et al. Induction of mitochondrial biogenesis is a maladaptive mechanism in mitochondrial cardiomyopathies. *J Am Coll Cardiol*. 2007;50(14):1362-9.
63. Zweier JL, Talukder MA. The role of oxidants and free radicals in reperfusion injury. *Cardiovasc Res*. 2006 May 1;70(2):181-90.

64. Bak MI, Ingwall JS. NMR-invisible ATP in heart: Fact or fiction? *Am J Physiol*. 1992 Jun;262(6 Pt 1):E943-7.
65. Shen W, Xu X, Ochoa M, Zhao G, Wolin MS, Hintze TH. Role of nitric oxide in the regulation of oxygen consumption in conscious dogs. *Circ Res*. 1994 Dec;75(6):1086-95.
66. Brown GC. Nanomolar concentrations of nitric oxide reversibly inhibit synaptosomal respiration by competing with oxygen at cytochrome oxidase. *FEBS Lett*. 1994;356(2-3):295-8.
67. Melino G, Bernassola F, Knight RA, Corasaniti MT, Nistico G, Finazzi-Agro A. S-nitrosylation regulates apoptosis. *Nature*. 1997 Jul 31;388(6641):432-3.
68. Ghatan S, Larner S, Kinoshita Y, Hetman M, Patel L, Xia Z, et al. p38 MAP kinase mediates bax translocation in nitric oxide-induced apoptosis in neurons. *J Cell Biol*. 2000 Jul 24;150(2):335-47.
69. Elrod JW, Wong R, Mishra S, Vagnozzi RJ, Sakthivel B, Goonasekera SA, et al. Cyclophilin D controls mitochondrial pore - dependent Ca^{2+} exchange, metabolic flexibility, and propensity for heart failure in mice. *J Clin Invest*. 2010;120(10):3680-7.
70. Kroemer G, Galluzzi L, Brenner C. Mitochondrial membrane permeabilization in cell death. *Physiol Rev*. 2007 Jan;87(1):99-163.
71. Vieira HLA, Belzacq A-, Haouzi D, Bernassola F, Cohen I, Jacotot E, et al. The adenine nucleotide translocator: A target of nitric oxide, peroxynitrite, and 4-hydroxynonenal. *Oncogene*. 2001;20(32):4305-16.
72. Szewczyk A, Wojtczak L. Mitochondria as a pharmacological target. *Pharmacological Reviews*. 2002;54(1):101-127.
73. Szeto HH. Mitochondria-targeted cytoprotective peptides for ischemia-reperfusion injury. *Antioxidants and Redox Signaling*. 2008;10(3):601-19.
74. Neuzil J, Widén C, Gellert N, Swettenham E, Zabalova R, Dong L-, et al. Mitochondria transmit apoptosis signalling in cardiomyocyte-like cells and isolated hearts exposed to experimental ischemia-reperfusion injury. *Redox Report*. 2007;12(3):148-62.
75. Cho J, Won K, Wu D, Soong Y, Liu S, Szeto HH, et al. Potent mitochondria-targeted peptides reduce myocardial infarction in rats. *Coron Artery Dis*. 2007;18(3):215-20.
76. Gane EJ, Weilert F, Orr DW, Keogh GF, Gibson M, Lockhart MM, et al. The mitochondria-targeted anti-oxidant mitoquinone decreases liver damage in a phase II study of hepatitis C patients. *Liver International*. 2010;30(7):1019-26.
77. Bayeva M, Ardehali H. Mitochondrial dysfunction and oxidative damage to sarcomeric proteins. *Curr Hypertens Rep*. 2010;12(6):426-32.

78. Murphy MP, Smith RAJ. Targeting antioxidants to mitochondria by conjugation to lipophilic cations [Internet]; 2007 [cited 23 April 2013].
79. Snow BJ, Rolfe FL, Lockhart MM, Frampton CM, O'Sullivan JD, Fung V, et al. A double-blind, placebo-controlled study to assess the mitochondria-targeted antioxidant MitoQ as a disease-modifying therapy in parkinson's disease. *Movement Disorders*. 2010;25(11):1670-4.
80. Smith RAJ, Porteous CM, Gane AM, Murphy MP. Delivery of bioactive molecules to mitochondria in vivo. *Proc Natl Acad Sci U S A*. 2003;100(9):5407-12.
81. Winterbourn CC, Parsons-Mair HN, Gebicki S, Gebicki JM, Davies MJ. Requirements for superoxide-dependent tyrosine hydroperoxide formation in peptides. *Biochem J*. 2004 Jul 1;381(Pt 1):241-8.
82. Zhao K, Zhao G-, Wu D, Soong Y, Birk AV, Schiller PW, et al. Cell-permeable peptide antioxidants targeted to inner mitochondrial membrane inhibit mitochondrial swelling, oxidative cell death, and reperfusion injury. *J Biol Chem*. 2004;279(33):34682-90.
83. Zhao K, Luo G, Zhao GM, Schiller PW, Szeto HH. Transcellular transport of a highly polar 3+ net charge opioid tetrapeptide. *J Pharmacol Exp Ther*. 2003 Jan;304(1):425-32.
84. Lave T, Dupin S, Schmitt C, Valles B, Ubeaud G, Chou RC, et al. The use of human hepatocytes to select compounds based on their expected hepatic extraction ratios in humans. *Pharm Res*. 1997 Feb;14(2):152-5.
85. Rocha M, Hernandez-Mijares A, Garcia-Malpartida K, Bañuls C, Bellod L, Victor VM. Mitochondria-targeted antioxidant peptides. *Curr Pharm Des*. 2010;16(28):3124-31.
86. Zhao K, Zhao GM, Wu D, Soong Y, Birk AV, Schiller PW, et al. Cell-permeable peptide antioxidants targeted to inner mitochondrial membrane inhibit mitochondrial swelling, oxidative cell death, and reperfusion injury. *J Biol Chem*. 2004 Aug 13;279(33):34682-90.
87. Cho S, Szeto HH, Kim E, Kim H, Tolhurst AT, Pinto JT. A novel cell-permeable antioxidant peptide, SS31, attenuates ischemic brain injury by down-regulating CD36. *J Biol Chem*. 2007 Feb 16;282(7):4634-42.
88. Blakeman N, Chen Q, Tolson J, Rueter B, Diaz B, Casey B, et al. Triacsin C, a fatty acyl CoA synthetase inhibitor, improves cardiac performance following global ischemia. *American Journal of Biomedical Sciences*. 2012;4(3):249,250-261.
89. Peterman EE, Taormina P, 2nd, Harvey M, Young LH. Go 6983 exerts cardioprotective effects in myocardial ischemia/reperfusion. *J Cardiovasc Pharmacol*. 2004 May;43(5):645-56.

90. Phillipson A, Peterman EE, Taormina P, Jr, Harvey M, Brue RJ, Atkinson N, et al. Protein kinase C-zeta inhibition exerts cardioprotective effects in ischemia-reperfusion injury. *Am J Physiol Heart Circ Physiol*. 2005 Aug;289(2):H898-907.
91. Omiyi D, Brue RJ, Taormina P, 2nd, Harvey M, Atkinson N, Young LH. Protein kinase C beta11 peptide inhibitor exerts cardioprotective effects in rat cardiac ischemia/reperfusion injury. *J Pharmacol Exp Ther*. 2005 Aug;314(2):542-51.
92. Bederson JB, Pitts LH, Germano SM, Nishimura MC, Davis RL, Bartkowski HM. Evaluation of 2,3,5-triphenyltetrazolium chloride as a stain for detection and quantification of experimental cerebral infarction in rats. *Stroke*. 1986 Nov-Dec;17(6):1304-8.
93. Adegboyega PA, Adesokan A, Haque AK, Boor PJ. Sensitivity and specificity of triphenyl tetrazolium chloride in the gross diagnosis of acute myocardial infarcts. *Arch Pathol Lab Med*. 1997 Oct;121(10):1063-8.
94. Li G, Dai G, Xiang B, Mark J, Tomanek B, Liu H, et al. Mapping myocardial viability using interleaved T1-T2 weighted imaging. *Int J Card Imaging*. 2004;20(2):135-43.
95. Kloner RA, Hale SL, Dai W, Gorman RC, Shuto T, Koomalsingh KJ, et al. Reduction of ischemia/reperfusion injury with bendavia, a mitochondria-targeting cytoprotective peptide. *J Am Heart Assoc*. 2012 Jun;1(3):e001644.
96. Inagaki K, Hahn HS, Dorn GW, 2nd, Mochly-Rosen D. Additive protection of the ischemic heart ex vivo by combined treatment with delta-protein kinase C inhibitor and epsilon-protein kinase C activator. *Circulation*. 2003 Aug 19;108(7):869-75.
97. Savage RM, Guth B, White FC, Hagan AD, Bloor CM. Correlation of regional myocardial blood flow and function with myocardial infarct size during acute myocardial ischemia in the conscious pig. *Circulation*. 1981 Oct;64(4):699-707.
98. Chandran K, Aggarwal D, Migrino RQ, Joseph J, McAllister D, Konorev EA, et al. Doxorubicin inactivates myocardial cytochrome c oxidase in rats: Cardioprotection by mito-Q. *Biophys J*. 2009;96(4):1388-98.
99. Galbreath T, Chen Q, Ondrasik R, Bertolet M, Barsotti R, Young LH. Effects of mitochondrial-targeted antioxidants on real-time nitric oxide and hydrogen peroxide release in hind Limb Ischemia and reperfusion (I/R). *Peptides Across the Pacific: The Proceedings of the Twenty-Third American and Sixth International Peptide Symposium*. 2013:46-7.
100. Graham D, Huynh NN, Hamilton CA, Beattie E, Smith RAJ, Cochemé HM, et al. Mitochondria-targeted antioxidant mitoq10 improves endothelial function and attenuates cardiac hypertrophy. *Hypertension*. 2009;54(2):322-8.
101. Dhanasekaran A, Kotamraju S, Kalivendi SV, Matsunaga T, Shang T, Keszler A, et al. Supplementation of endothelial cells with mitochondria-targeted antioxidants inhibit

peroxide-induced mitochondrial iron uptake, oxidative damage, and apoptosis. *J Biol Chem.* 2004 Sep 3;279(36):37575-87.

102. Ondrasik R, Chen Q, Navitsky K, Chau W, Devine I, Lau OS, et al. Cardioprotective effects of mitochondrial-targeted antioxidants in myocardial ischemia/reperfusion (I/R) injury. *Peptides Across the Pacific: The Proceedings of the Twenty-Third American and Sixth International Peptide Symposium.* 2013:64-5.

103. Cassarino DS, Parks JK, Parker Jr. WD, Bennett Jr. JP. The parkinsonian neurotoxin MPP+ opens the mitochondrial permeability transition pore and releases cytochrome c in isolated mitochondria via an oxidative mechanism. *Biochimica et Biophysica Acta - Molecular Basis of Disease.* 1999;1453(1):49-62.

104. Song W, Shin J, Lee J, Kim H, Oh D, Edelberg JM, et al. A potent opiate agonist protects against myocardial stunning during myocardial ischemia and reperfusion in rats. *Coron Artery Dis.* 2005 Sep;16(6):407-10.

105. Orrenius S. Reactive oxygen species in mitochondria-mediated cell death. *Drug Metab Rev.* 2007;39(2-3):443-55.

106. Whiteman M, Spencer JP, Szeto HH, Armstrong JS. Do mitochondriotropic antioxidants prevent chlorinative stress-induced mitochondrial and cellular injury? *Antioxid Redox Signal.* 2008 Mar;10(3):641-50.

107. Han Z, Varadharaj S, Giedt RJ, Zweier JL, Szeto HH, Alevriadou BR. Mitochondria-derived reactive oxygen species mediate heme oxygenase-1 expression in sheared endothelial cells. *J Pharmacol Exp Ther.* 2009 Apr;329(1):94-101.

108. Yang L, Zhao K, Calingasan NY, Luo G, Szeto HH, Beal MF. Mitochondria targeted peptides protect against 1-methyl-4-phenyl-1,2,3,6- tetrahydropyridine neurotoxicity. *Antioxidants and Redox Signaling.* 2009;11(9):2095-104.

109. Fonck C, Baudry M. Rapid reduction of ATP synthesis and lack of free radical formation by MPP+ in rat brain synaptosomes and mitochondria. *Brain Res.* 2003 Jun 13;975(1-2):214-21.

110. Fenton RA, Dickson EW, Meyer TE, Dobson JG, Jr. Aging reduces the cardioprotective effect of ischemic preconditioning in the rat heart. *J Mol Cell Cardiol.* 2000 Jul;32(7):1371-5.

111. Przyklenk K, Li G, Simkhovich BZ, Kloner RA. Mechanisms of myocardial ischemic preconditioning are age related: PKC-epsilon does not play a requisite role in old rabbits. *J Appl Physiol.* 2003 Dec;95(6):2563-9.